N2O flux measurements over an irrigated maize crop: A comparison of three methods

Tiphaine Tallec, Aurore Brut, Lilian Joly, Nicolas Dumelié, Dominique Serça, Patrick Mordelet, Nicole Claverie, D. Legain, J. Barrié, T. Decarpenterie, et al.

N_2O flux measurements over an irrigated maize crop: A comparison of three methods

T. Tallec[a,*], A. Brut[a], L. Joly[b], N. Dumelié[b], D. Serça[c], P. Mordelet[a], N. Claverie[a], D. Legain[d], J. Barrié[d], T. Decarpenterie[b], J. Cousin[b], B. Zawilski[a], E. Ceschia[a], F. Guérin[e], V. Le Dantec[a]

[a] *Centre d'Etudes Spatiales de la BIOsphère, UMR 5126 CNES/CNRS/IRD/UPS, 18 avenue Edouard Belin, 31401, Toulouse, France*
[b] *Groupe de Spectrométrie Moléculaire et Atmosphérique GSMA, Université de Reims-Champagne Ardenne, UMR 7331 URCA/CNRS, Moulin de la Housse, BP 1039, 51687, Reims, France*
[c] *Laboratoire d'Aérologie, OMP, UMR 5560 UPS/CNRS, 14 avenue Edouard Belin, 31400, Toulouse, France*
[d] *Groupe d'étude de l'Atmosphère Météorologique, Centre National de Recherches Météorologiques, UMR 3589, Météo, France*
[e] *Geosciences Environnement Toulouse UMR 5563 & UR 234 IRD, Université Paul Sabatier, Avenue Edouard Belin 14, Toulouse, 31400, France*

This paper presents the NitroCOSMES campaign, aimed at testing and evaluating the performance of three methods for monitoring N_2O fluxes over an agricultural field. The experiment was conducted from May to August 2012 at a site located in the south-west of France. N_2O fluxes from a 24 ha irrigated maize field were measured using eddy covariance (EC), automated chamber (AC) and static chamber (SC) methodologies. Uncertainties were calculated according to the specificities of each set-up. Measurements were performed over a large range of water-filled pore spaces (WFPS), soil temperatures, and mineral nitrogen availability, and offered the opportunity to compare methodologies over a wide range of N_2O emission intensities. The average N_2O fluxes were compared among the three methodologies during the same periods of measurement and for different intensities of emissions (low, moderate and high). Periods of comparison were determined according to the AC results. On average, the three methods gave comparable results for the low (SC: 14.7 ± 2.2, EC: 15.7 ± 10.1, AC: 17.5 ± 1.6 ng N_2O-N m^{-2} s^{-1}) and the high (SC: 131.7 ± 22.1, EC: 125.3 ± 8, AC: 125.1 ± 8.9 ng N_2O-N m^{-2} s^{-1}) N_2O emission ranges. For the moderate N_2O emission range, AC measurements gave higher emis-sions (57.2 ± 3.9 ng N_2O-N m^{-2} s^{-1}) on average than both the SC (41.6 ± 6.6 ng N_2O-N m^{-2} s^{-1}) and EC (33.8 ± 3.9 ng N_2O-N m^{-2} s^{-1}) methods, which agreed better with each other. The relative standard deviation coefficient (RSD) indicated that EC methodology gave highly variable values during periods of low N_2O emis-sions, from -52.2 ± 88.1 to 62.2 ± 50.7 ng N_2O-N m^{-2} s^{-1}, with a mean RSD of 151%. Water vapour effects (dilution and spectroscopic cross-sensitivity) were discussed in an attempt to explain the high variability in low N_2O emission measurements. Even after applying the Webb term correction, there could still be a spectroscopic cross-sensitivity effect of water vapour on the N_2O trace gas signal because of the layout of the analysers, which was not determined during the experiment. This study underlined that EC methodology is a promising way to estimate and refine N_2O budgets at the field scale and to analyse the effects of different agricultural practices more finely with continuous flux monitoring. It also highlighted the need to continue the effort to assess and develop chambers and EC methodologies, especially for the low N_2O emission measurement range, for which values and systematic uncertainties remain high and highly variable.

1. Introduction

The need to assess the dynamics of greenhouse gas exchanges between land surface and atmosphere more accurately is of high priority. While carbon dioxide fluxes have been widely measured using the eddy-covariance method for many years (Baldocchi, 2014), continuous measurements of nitrous oxide (N_2O) fluxes remain scarce at the ecosystem scale (Nicolini et al., 2013). Since N_2O is estimated to account for 6% of the global greenhouse effect (Ciais et al., 2013), and the application of nitrogen fertilizers in agriculture is estimated to be responsible for more than half of the anthropogenic N_2O emissions (IPCC, 2006), the accurate evaluation N_2O emissions from croplands is critical.

* Corresponding author.
E-mail address: tiphaine.tallec@cesbio.cnes.fr (T. Tallec).

In a Europe-wide synthesis study performed on 17 different crop sites (51 years of CO_2 flux monitoring), Ceschia et al. (2010) pointed out that N_2O emissions (estimations based upon IPCC 2006 emission factor) had the potential to attenuate the CO_2 sink activity of croplands by 16%. Zenone et al. (2016) demonstrated that N_2O flux would offset 50% of the sink activity in a short rotation coppice used for bioenergy production and that accurate monitoring of the N_2O emission events was critical for deriving correct estimates of the GHG budget. Moreover, Smith et al. (2014) showed that strong potential levers exist for attenuating N_2O emissions from cropland. Nitrogen (N) fertilization modalities, plant (for N use efficiency) and water management appear as key levers in cropland. Although Lesschen et al. (2011) show that the emission factor can vary considerably according to the soil, climate, crop and management, the IPCC emission factor for estimating N_2O emissions remains widely used when N_2O fluxes cannot be monitored continuously. In most studies, N_2O flux measurements are performed using manual or automated chambers combined with a gas chromatograph or infrared analyser (Eugster and Merbold, 2015). Both chamber methodologies have the advantages of being cost effective and of addressing the issue of spatial variability on reported fluxes within the studied plot (Cowan et al., 2015). In addition, automated chambers have the advantage of monitoring N_2O fluxes more frequently with less dependence on manpower. They require less gap-filling than manual chambers, which are very demanding in manpower and introduce considerable uncertainty on calculations of the total annual N_2O budget when used at low sampling frequency (Crill et al., 2000; Smith and Dobbie, 2001; Barton et al., 2015). For both methodologies, one disadvantage is the uncertainty related to spatial and/or temporal sampling rates being too low (Barton et al., 2015), which may lead to skewed sampling of emissions over the whole range of spatial and temporal variation (under sampling of hot moments).

N_2O emissions from soils are known to vary rapidly in both space and time (Cowan et al., 2015). The exchanges of N_2O between agroecosystems and the atmosphere depend on complex interactions with the available substrate (nitrogen and carbon), as the feeding process on one side and the availability of oxygen on the other side determine the pathway that is taken in the nitrification or denitrification processes (Butterbach-Bahl et al., 2013). Hot spots of N_2O production in a plot are often due to high variability of the spatial distribution of organic matter and of texture components (clay particularly), heterogeneous residual crop incorporation, soil compaction, manure or slurry spreading and the area of waterlogged spots (Cowan et al., 2015). So far, measuring soil-atmosphere trace gas exchanges with high accuracy and adequate spatial representativeness of the whole field remains a challenge. In order to assess the effects of management and climate variability on net GHG budgets, methodologies are required that are more suitable for measuring GHG fluxes at the scale at which agroecosystems are managed, i.e. at the field scale. Micrometeorological methods are the most appropriate at such a scale. During the last decade, micrometeorological greenhouse gas measurements have become more common as an alternative to the traditional chamber ones (Pattey et al., 2007). With the availability of a new generation of fast analysers (Hensen et al., 2013; Rannik et al., 2015; Shurpali et al., 2016), an increasing number of investigations are being conducted on the use of the eddy covariance method to measure N_2O fluxes at the ecosystem and landscape scales (Bureau, 2017), although they still remain too scarce (Eugster and Merbold, 2015). The majority have been carried out on pasture sites and bio-energy plantations (Eugster et al., 2007; Neftel et al., 2010; Zona et al., 2013; Merbold et al., 2014; Rannik et al., 2015). The eddy covariance method has the advantage of continuously measuring and directly integrating flux data across a large area (> 100 m^2) without disturbing the soil or the interface between the surface and the atmosphere. However, the measurement of small N_2O flux events with the EC method is still very challenging because the N_2O gas analyser requires a much higher resolution to detect N_2O atmospheric fluctuations than is needed for CO_2 fluctuations, since the ratio between the concentrations of the two gases in the atmosphere is about 1000:1. To our knowledge, only a few studies assessing EC accuracy on N_2O flux measurements have been conducted on crops (Skiba et al., 1996; Molodovskaya et al., 2011; Wang et al., 2013; Huang et al., 2014). Moreover, Nicolini et al. (2013) have reported that few studies directly compare N_2O flux dynamics using chambers and EC methods over a long period of experimentation at crop plot scale. Most of them have been based on manual chambers, which are subject to large errors due to low frequency of measurement. According to the available studies, Nicolini et al. drew contrasted conclusions on the issue. Some case studies led to good agreement (Laville et al., 1999; Jones et al., 2011; Molodovskaya et al., 2011; Hargreaves et al., 1996; Wienhold et al., 1995) while a study carried out in Scotland resulted in poor agreement (differences of up to 200%) between the two methods (Galle et al., 1994; Hargreaves et al., 1994; Smith et al., 1994). Discrepancies between manual chambers and micrometeorological techniques were mostly due to the differences in the sampled area or spot sources generated by a drainage system within the crop plot, which manual chambers could not measure (Denmead et al., 2010). It is thus indisputable that eddy-covariance flux systems for N_2O measurement still require evaluation against reference methods with higher frequencies of measurement and longer periods of comparison. A longer period of comparison allows methods to be tested over a large range of variations in key environmental factors.

In this paper, we present the results of the NitroCOSMES project, which was conducted to compare four methods for measuring N_2O fluxes during a growing season over an irrigated maize field: automated chambers, manual chambers, eddy covariance and relaxed eddy accumulation (REA). Unfortunately, the REA method failed rapidly and we did not obtain relevant measurements from it for comparison, so it will not be presented in the following. In this paper, we describe and critically assess the three methods effectively used to measure N_2O fluxes and report results from 100 days of campaign. We postulated that both sets of chambers would capture the spatial heterogeneity of N_2O fluxes along with the area integrated by the EC method. We tested whether the EC method was sensitive enough to capture background N_2O fluxes and, above all, the temporal N_2O flux variability that the chamber methods are not able to monitor. We also suspected and analysed a possible effect of the automated chamber system on soil microclimate, compared to the non-intrusive EC system, and found that it probably created some artefacts in the measurement, inducing over- or under-estimation of the calculated N_2O fluxes.

2. Material and methods

2.1. The experimental site

The campaign to compare methodologies was conducted from 10 May to 18 August 2012 (100 days), on a flat agricultural field site of 24 ha located in the south-west of France, 30 km from the city of Toulouse (43°49′65″N, 01°23′79″E) at an altitude of 180 m above sea level. Located near the village of Lamasquère, the experimental site belongs to a dairy farm which is the property of the Purpan Engineering School (Beziat et al., 2009). The Lamasquère site (FR-Lam) is also part of the regional spatial observatory (OSR) and the European Research Infrastructure Consortium ICOS (Integrated Carbon Observation System). The soil is classified as clayey (54.3% clay, 33.7% loam, 12% sand). The mean organic carbon and total nitrogen soil contents of the 0–30 cm layer were 80 ton ha^{-1} and 8.8 ton ha^{-1}, respectively, during the campaign. Winter wheat had been sown in the previous year's rotation. Maize seeds were sown on April 27. The maize was irrigated 5 times during the growing season, fertilized with solid manure (145 kg N eq. per ha) in September 2011 and with mineral nitrogen (urea) once, on 20 May 2012 (110 kg N eq. per ha). Herbicide was applied on 15 May. N_2O flux measurements started on 10 May and ended on 18 August, thus covering the majority of the maize-growing season.

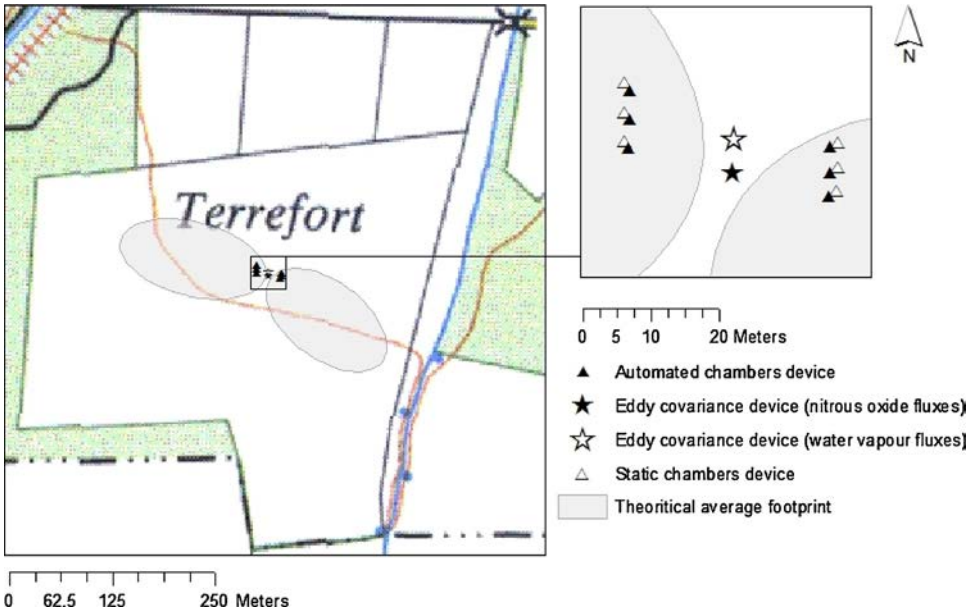

Fig. 1. Spatial distribution of devices for N_2O flux measurement on Lamasquère site.
The main characteristics of the 3 systems are summarized in Table 1 and a scheme of the devices implemented is given in Fig. 2.

During this experiment, automated and static chambers were set up close to each other and distributed within the fetch area of the EC system at 20 m from the EC flux tower so as to represent the area sampled by the EC system (Fig. 1).

2.2. N_2O flux measurement methodologies

2.2.1. Automated chamber measurements

N_2O flux measurements were performed with AC during the entire year 2012 using a set of six closed automated chambers distributed inside the footprint at a distance of about 15-20 m from the flux tower. The system circulated air at approximately 1 L.min^{-1} via an air pump between each chamber and two low frequency infrared gas analysers, one for measuring N_2O molar fraction (Thermofisher 46i, Megatec, France) and the other for measuring CO_2 molar fraction (LI820, LiCor, Lincoln, NE, USA). These relatively compact infrared gas analysers were used continuously to measure gas molar fractions within the dynamic chamber system (with a detection limit of approximately 0.02 and 0.5 ppm, and a precision of 1% and less than 3% on the reading for N_2O and CO_2 respectively). CO_2 molar fraction measurements, not described in this paper, were used to detect any leakage problems. Water vapour was not measured and no correction was made for the possible dilution effect. However, a recent experiment (data not shown, Zawilski) proved that the relative air humidity inside the chamber rapidly reached saturation (in 50 s) after closure. Once that delay had passed after closure, the ambient air saturation with water vapour was assumed to be maximum and thus to have the same impact on the molar fraction measurement in the various chambers. As the first five measurements (corresponding to the 50 s delay) were not taken into account in the model fit for the flux calculation, any possible difference of dilution effect on the N_2O molar fraction and so on the resulting exponential adjustment was considered negligible and no correction was made for it.

The stainless steel chambers had horizontal dimensions of 0.23 x 0.7 m, covering an area of 0.161 m^2, and a height of 0.227 m. The chambers were inserted 0.05-0.10 m into the soil. Their dimensions allowed the chambers to be inserted in the crop interrows (varying between 0.16 and 0.8 m), thus minimizing vegetation disturbance around the chambers and providing an acceptable integration of the flux heterogeneity at fine scale (Bessou et al., 2010). For a complete description of the system, see Peyrard et al. (2016).

N_2O molar fraction measurements were taken every 6 h, at 00:00, 06:00, 12:00 and 18:00, i.e. four measurement cycles per day. At the beginning and end of each cycle, the N_2O molar fraction of the ambient air was measured at one metre above the ground with a tube inlet, in order to detect any possible drift of the analyser and to assess the accuracy of the measured gas concentration during the full measuring cycle. In between, potential N_2O accumulation was measured sequentially in each chamber. Each period of measurement was preceded by a purge of 2 min in order to eliminate any gas remaining inside the pipes and analyser from the previous measurement. For each chamber, the measuring cycle took 17.5 min. Chambers were removed from their location before each field operation (tillage, irrigation, fertilization, herbicide application and harvest) and then replaced, resulting in some significant periods without measurements (see results).

To calculate the N_2O fluxes, the data were previously fitted, after a delay of 50 s of measurement, with a rising exponential regression model. The delay of 50 s was chosen in order to avoid the calculated fluxes being influenced by any effect related to physical disturbance caused by the chamber closure.

N_2O fluxes per chamber ($F_{N2O\text{-}chamber}$, expressed in ng N_2O-N m^{-2} s^{-1}) were then calculated from the previously determined slope and following Peyrard et al. (2016):

$$F_{N2O-chamber} = \frac{h \times M_m}{V_m}\left(\frac{dC}{dt}\right)_{t=t}0 \quad (1)$$

where h is the headspace height (cm), M_m is the molar weight of N in N_2O (M_m = 28 g mol^{-1}), V_m is the molar volume in standard conditions (24.1 L mol^{-1} at 20 °C) and $\left(\frac{dC}{dt}\right)_{t=t_0}$ is the slope (in ppb) obtained from the regression of concentration vs. time at t_0 (i. e. 50 s after chamber closure). $F_{N2O\text{-}chamber}$ were filtered by means of a mixture of goodness-of-fit statistics and visual inspection.

The N_2O flux detection limit over the 17.5 min cycle was estimated according to the method described by Neftel et al. (2007) and was equal to 4.52 ng N_2O m^{-2} s^{-1}.

To compare N_2O fluxes between EC and chamber systems, we calculated the mean F_{N2O} per cycle ($F_{N2O\text{-}cycle}$) provided that at least three of the possible six $F_{N2O\text{-}chamber}$ were available for each measuring cycle. For comparison between chambers, $F_{N2O\text{-}day}$ were calculated provided that at least two of the possible four $F_{N2O\text{-}cycle}$ were available for

calculation. These choices for mean flux computation were verified statistically. For cycles with six $F_{N2O\text{-}chamber}$ values, we tested the computation of $F_{N2O\text{-}cycle}$ using data from only three $F_{N2O\text{-}chamber}$. For each cycle, three values were drawn at random using the algorithm developed by Wichman and Hil (1987) that is implemented in Excel 2010. Then the means of $F_{N2O\text{-}cycle}$ computed using these three values of $F_{N2O\text{-}chamber}$ were compared with those computed using the six $F_{N2O\text{-}chamber}$ to calculate the deviation due to this choice of using three of the six $F_{N2O\text{-}chamber}$. This procedure was performed four times. On average, we found a deviation of 8%, with a minimum of 2% and a maximum of 16%. This result justified our choice of calculating $F_{N2O\text{-}cycle}$ with at least three $F_{N2O\text{-}chamber}$ so as to keep a maximum of data and optimize the representativeness for temporal and spatial distribution of the N_2O fluxes.

Uncertainty in an $F_{N2O\text{-}cycle}$ was calculated using the random error calculation:

$$U_{FN2O-cycle} = \frac{SD}{\sqrt{n}} \quad (2)$$

where *SD* is the standard deviation and n is the number of $F_{N2O\text{-}chamber}$ values.

The random uncertainty propagated in a mean flux range (U_{range}) was estimated using Eq. (3):

$$U_{range-chamber} = \frac{\sqrt{\sum U_{FN\,2O-cycle}^2}}{n} \quad (3)$$

2.2.2. Static chamber measurements

A set of 6 static chambers was used to monitor N_2O accumulation inside the chamber and thus calculate N_2O fluxes. Chambers were positioned on collars that were inserted 10 cm deep in the soil two days prior to the measurements to avoid any disturbances. Chambers were made airtight by filling a slot at the top of the collar with water (Mazzetto et al., 2014). The 6 collars were installed around the EC tower in the footprint close to the automated chambers. Air samples (20 mL) were collected immediately after the chamber was closed and then every 15 min for the next 45 min. Samples for N_2O analysis were stored in serum vials initially filled with a salt-saturated solution as described in Deshmukh et al. (2014). The analyses were carried out later by gas chromatography (GC) in the laboratory. N_2O concentration was determined in the sample headspace with an SRI 8610C gas chromatograph (Torrance, CA, USA), equipped with an Electron Capture Detector (ECD). The gas chromatograph was calibrated for every ten samples using commercial gas standards (300 and 1000 ppbv, Air Liquide "Crystal®" standards). Duplicate injection of samples (0.5 mL) showed reproducibility that was always better than 5%. For the SC methodology fluxes were calculated from the slope of a linear regression of N_2O concentration in the chamber versus time and following Eq. (1). Fluxes were rejected when the coefficient of determination r^2 was lower than 0.4. Days of N_2O flux measurements with the static chambers were chosen according to soil N_{min} availability and WFPS conditions in an attempt to capture the different ranges of N_2O emissions. The measurements were finally carried out on 4 days during the comparison experiment (11 and 24 May, 6 June, 1 July), when N_2O fluxes were of low, medium and high magnitude. During this measurement stage, a measurement protocol was performed from 2 to 3 times a day on each chamber, giving a potential total of 18 N_2O flux measurements a day. Random uncertainties per cycle and per range were calculated using Eqs. (2) and (3).

2.2.3. Relaxed eddy accumulation methodology

During the campaign, a Relaxed Eddy Accumulation method was implemented to simultaneously measure half-hourly N_2O fluxes, using an innovative and accurate Quantum Cascade Laser sensor (QCL), developed by GSMA (Groupe de Spectrometrie Moleculaire et Atmosphérique, Université de Reims), and H_2O and CO_2 fluxes, using the Li6262 (Campbell Scientific). The QCL prototype was also used to measure N_2O flux with the Eddy Covariance method and this instrument was, therefore, shared between the two techniques. Unfortunately, the REA system failed to provide good estimates for all fluxes because of an unsolved problem on the air conditional sampling part. Therefore, in this paper, we neither describe this methodology (see Businger and Oncley, 1990) nor present its results. Instead, the functioning diagram of the ECOFLUX station is displayed in Fig. (1) to contribute to the understanding of the different time stages of N_2O analysis.

2.2.4. Eddy covariance flux measurements

2.2.4.1. Set up. The N_2O and sensible heat EC measurements were carried out by combining a three-dimensional sonic anemometer (Gill Instruments, Lymington, UK, Model HS50) with a closed path QCLAS trace gas analyser developed by the GSMA laboratory, 20 cm apart. Data were recorded at a frequency of 10 Hz on a computer inside the ECOFLUX station.

The water vapour EC measurements, needed for WPL correction (Webb et al., 1980), were conducted in parallel over the same period, using the historical EC set-up on site. This consisted of a three-dimensional sonic anemometer (CSAT3, Campbell Scientific Inc., Logan, UT, USA) and a rapid open-path infrared gas analyser (LI-7500, LiCor, Lincoln, NE, USA) 15 cm apart (Beziat et al., 2009). Data were recorded at a frequency of 20 Hz on a data logger (CR3000, Campbell Scientific Inc., Logan, UT, USA).

Both masts were installed in the middle of the field in order to optimize the fetch in the main wind directions. EC instruments were mounted 3.65 m above the soil surface. There was a distance of 4 m between the EC systems. The height of the devices was chosen to be about 1 m higher than the crop at its maximum

2.2.4.2. QCLAS/ECOFLUX presentation. The ECOFLUX station was developed by GSMA to provide a mobile, autonomous system able to measure greenhouse gas fluxes using the eddy covariance technique. It performs continuous measurements in the field with temperature conditions ranging from -20 °C up to + 45 °C. The ECOFLUX platform comprises 5 specific parts:

1) The Quantum Cascade Laser Absorption Spectrometry (QCLAS) sensor, developed to precisely measure N_2O concentration with a sensitivity < 0.5 ppb and at high acquisition frequency (10 Hz) (Joly et al., 2011; Mappe et al., 2013; Mappe-Fogaing et al., 2012). The QCLAS principle is based on Beer Lambert's law (Eq. (4)).

$$I = I_0 \exp(-C \times \sigma \times L) \quad (4)$$

This law describes the absorption of light by a gas concentration during its propagation along an optical path *L*. *I* and I_0 correspond to the intensity of the transmitted radiation at the sample cell output and the intensity of the incident radiation, respectively. *C* is the concentration of the analysed gas (mol cm^{-3}), while σ is the absorption cross section of the transition. The simultaneous measurement of temperature and pressure inside the analyzer cell allowed converting the gas concentration into molar fraction. The gas is collected in a cell through a Synflex hose, which reduces the exchanges between the air and the sampling tube. The pumping flow rate is 15 L min^{-1}, which ensures a turbulent regime and a renewal of the sample chamber gas approximately every 100 ms.

2) The Vaisala WTX510 weather probe, which measures the meteorological parameters (atmospheric pressure, air temperature and humidity, rainfall information) at a frequency of 0.1 Hz.
3) A 3D windsonic (HS-50 Wind Meter by Gill Instruments) to record the three wind speed components at a frequency of about 50 Hz. Wind speed measurements were then synchronized with the N_2O

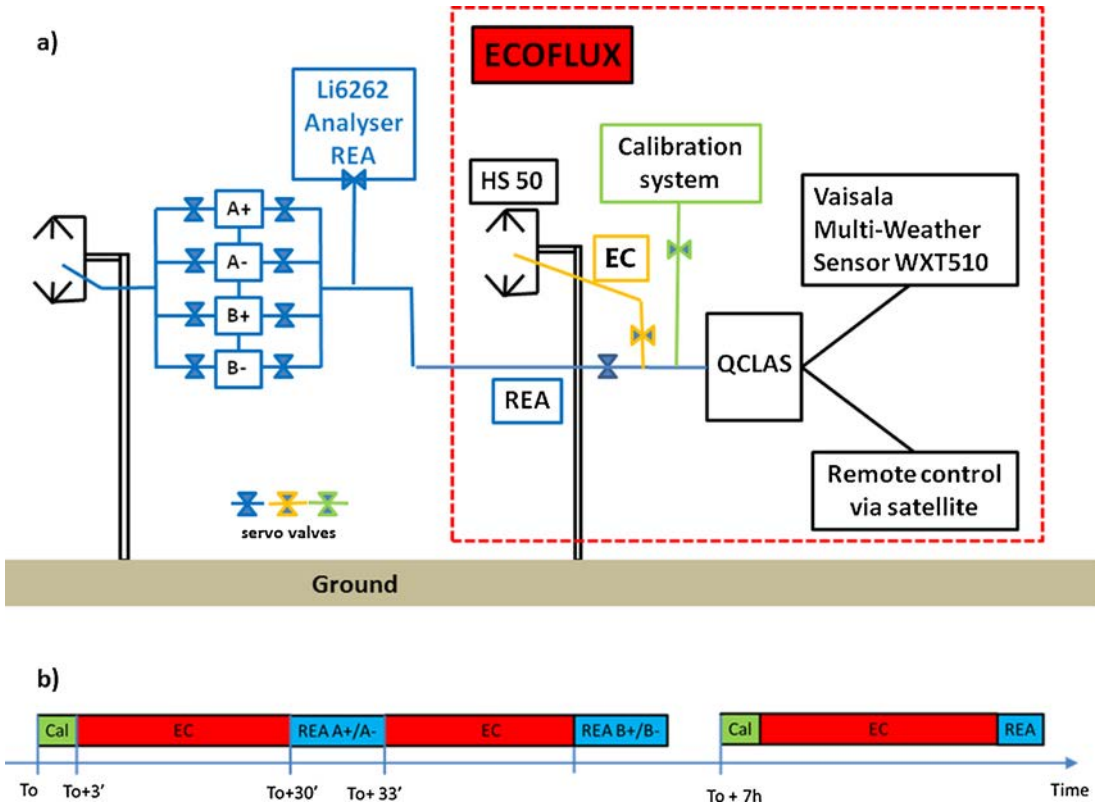

Fig. 2. a) Functioning diagram of the ECOFLUX station coupled with the REA and EC system during the campaign. b) Chronogram of the time stages of the Quantum Cascade Laser Absorption Spectrometry Sensor (QCLAS) measurements.

concentration measurements and both were recorded at the height of 3.65 m above the soil.

4) The satellite communication, which both remotely retrieves data from all sensors and remotely controls the system when necessary.
5) A calibration system that compensates for possible drifts of the instruments using three standard gas cylinders (307.33 ± 0.11 ppb; 324.46 ± 0.09 ppb and 354.53 ± 0.15 ppb) provided by NOAA. As the QCLAS measured N_2O concentrations for both EC and REA set-ups, we used a servo vacuum valve system, also controlled by QCLAS, to switch between the different kinds of analysis: REA, EC or calibration.

Fig. 2a shows the functioning diagram of the ECOFLUX station coupled with both the REA and the EC systems. Fig. 2b is a chronogram that illustrates the different time stages of the QCLAS. A calibration cycle occurs every 7 h so as to avoid any drift during the measurement campaign. A calibration phase lasts for 3 min. During this period, the 3 standard bottles are analysed. Apart from this calibration procedure, ECOFLUX is dedicated to N_2O measurements for the EC system for 27 min, before shifting to the REA system for the remaining 3 min to analyse the air contained in the pair of bags of the REA system.

The calibration system performed well during the campaign and the average sensitivity for all calibrations was less than 0.3 ppb (< 0.1%). In addition, differences between the measured mean concentration value and the NOAA standards were 0.2%, 0.25% and 0.06% for the 3 bottles. These results obtained in real field conditions allowed us to conclude that the ECOFLUX station estimates the absolute N_2O concentration accurately, even at a frequency of 10 Hz.

During the campaign, the cross-sensitivity of the N_2O analyser to water vapour was unfortunately not determined as recommended in Neftel et al. (2010). Neftel et al. determined a linear water interference of 0.3 ppb of dry N_2O per percentage point of relative humidity. They suggested that the magnitude of the analyser cross-sensitivity may depend on the specific instrument configuration and should be determined empirically. As there was no possible correction for that experiment, the issue is discussed.

2.2.4.3. Flux and uncertainties calculation. The EdiRe software (Robert Clement, © 1999, University of Edinburgh, UK) was used to calculate fluxes following CarboEurope-IP recommendations. Water vapour fluxes were calculated as the mean covariance between fluctuations of vertical wind speed and the density of water vapour in the air. N_2O fluxes ($F_{N2O\text{-}EC}$) were computed in a similar manner using the average covariance between fluctuations of vertical wind speed (w') and the molar fraction of N_2O (c') in the air. The time of the correlation peak, i.e. the lag time if a cross correlation occurred, was estimated. The time lag between c' and w' was estimated by means of correlation maximization in a time window of 3 ± 3 s, using their covariance and standard deviations. A mean time lag of 4.3 s was detected and used as the default value if no cross correlation was found or if it was equal to zero between the two signals. Fluctuations were obtained by subtracting the 30-minutes block average value from the instantaneous value (recorded at 10 Hz) (Reynolds decomposition). Before the flux calculation, spike detection (Vickers and Mahrt, 1997a,b) was applied to the measured variables, and a two-dimensional coordinate rotation (Kaimal and Finnigan, 1994) was performed on the wind components. The N_2O flux correction for the density fluctuation due to temperature was unnecessary as temperature fluctuations were damped by the long tube and, particularly, as a constant temperature and pressure were maintained in the sampling cell. However the N_2O flux correction for the density fluctuation due to dilution effect of water vapour was necessary as the sampled air was not dried prior to the concentration analysis in the sampling cell (Webb et al., 1980). The dilution effect is the change in the mole fraction of nitrous oxide measured by QCLAS which is artificially caused by variability in the water vapour content of the sampling air and not

due to a real change in the N_2O mole number. We derived the Webb correction term (χ_{webb}) using the water vapour flux data provided by the LI-7500/CSAT3 EC system. The Webb correction based on this open path EC system would overestimate the correction because damping of concentration and water vapour fluctuations had already taken place in the 5 m inlet tube of the closed EC system. So the cospectra of the water vapour flux inside the measurement cell of the QCLAS analyser was simulated (with Edire software) by decreasing the free atmospheric cospectra with the inverted transfer functions for cell volume averaging and tube attenuation. After water vapour dilution effect correction, half-hourly fluxes were corrected for spectral frequency loss (Moore, 1986). Flux filtering and quality controls were performed following the CarboEurope-IP recommendations. The integral turbulence characteristic (ITC) and steady state tests (Foken and Wichura, 1996) were applied to flag the quality of turbulence data. The ITC test consisted of comparing the measured and modelled ratios of the standard deviation of a turbulence parameter (w') and its turbulent flux (friction velocity U*). If the relative difference between them was higher than 100%, the half-hourly values were also rejected. The steady state test consisted of comparing the statistical parameters determined for the averaging period (30 min) and for shorter intervals (5 min) within this period. As proposed by Foken and Wichura (1996) if the difference between both covariances was higher than 30%, the time series was not steady state and then the associated calculated flux was filtered.

Using a night-time data analysis, we determined and applied a threshold of 0.1 m s^{-1} for the friction velocity U*below which we rejected the flux measurement. Finally, we checked the fetch with the footprint model from Kormann and Meixner (2001).

The 30-minutes value was rejected when less than 90% of the flux came from the crop site. The system flux detection limit was then estimated using the methodology proposed by Wang et al. (2013). In this study, the noise level of the QCLAS for N_2O (ppbv) was set at 0.5 ppbv, and the mean standard deviation of the vertical wind velocity during the measurement period was approximately 0.31 m s^{-1}. For an averaging period of 30 min, the detection limit of the N_2O fluxes was 8.2 ng N_2O m^{-} s^{-1}.

As concentration profiles of N_2O were not measured, no storage term was added to the final calculation of the N_2O fluxes.

Systematic flux uncertainties were calculated according to Kroon et al. (2010) and Wang et al. (2013), who highlighted that the uncertainties were mainly caused by the uncertainty due to one-point sampling (U_{op}). This uncertainty contributed more than 90% on average to the total uncertainty, especially when N_2O fluxes were of high magnitude in our case. We also calculated and added systematic uncertainty due to the Webb correction (U_{webb}) since the N_2O dry mixing ratio was not measured and the sampled air was not dried prior to measurement inside the cell. Combining the two terms gave an estimate of the systematic uncertainty as follows:

$$U_{EC} = \sqrt{(U_{op})^2 + (U_{webb})^2} \quad (5)$$

$$\text{with } U_{op} = \sqrt{\frac{20z}{TU}}\sqrt{\overline{(w'c')^2} - (\overline{w'c'})^2}$$

$$U_{webb} = \sqrt{(\chi_{webb}\sqrt{(0.2)^2 + (\sqrt{200z/TU})^2})^2}$$

and $\chi_{webb} = \lambda E \times 0.649 \times 10^{-6}\left(\frac{\bar{\rho}_{N_2O}}{\bar{\rho}_{air}}\right)$ where T is the averaging time in seconds, U is the wind speed in m s^{-1}, z is the height measurement in metres, $\bar{\rho}_{N_2O}$ and $\bar{\rho}_{air}$ are the mean densities of N_2O and air in kg m^{-3}, λE is the latent heat flux in W m^{-2}, w' and c' are the instantaneous deviations of the vertical wind velocity (m s^{-1}) and the N_2O concentration (nmol mol^{-1}), respectively, from the mean values. χ_{webb} is the water vapour Webb correction term.

The systematic uncertainty in a mean-range flux ($U_{range\text{-}EC}$) was estimated using:

$$U_{range-EC} = \frac{\sqrt{\sum U_{EC}^2}}{n} \quad (6)$$

where n is the number of $F_{N2O\text{-}EC}$ samples.

2.3. Additional measurements

A weather station was used to record 30-minutes precipitation, air temperature and pressure, wind speed and direction, air relative humidity, and solar radiation. The annual mean temperature and precipitation over the past nine years were 13.13 °C and 598.5 mm, respectively. With a mean wind speed of 1.79 m s^{-1}, the prevailing wind directions at the field site were from the west-north-west and east-south-east with a fetch of over 200 and 140 m, respectively, i.e. inside the field perimeter.

Volumetric soil water content and temperature were monitored every hour at 0–7 cm depth inside each automated chamber (ML2x Thetaprobes, T107 thermistors) and every half-hour at 3 locations outside the chambers but inside the footprint. As water filled pore space (WFPS) is a key variable for microbial activity, and an indirect proxy of N_2O production and diffusion, it was calculated from the volumetric soil water content measured in the 0–7 cm layer and the soil characteristics, using Eq. (7).

$$WFPS = \frac{\theta_w}{1 - \frac{D_b}{D_p}} \quad (7)$$

with θ_w the volumetric soil water content in percent, D_p the soil particle density, assumed to be 2.6 g/cm^3, D_b the soil bulk density. Bulk density was not monitored and therefore an accurate WFPS could not be calculated. We analysed the sensitivity of WFPS to bulk density between 1.05 and 1.45, corresponding to the measured minimum (after tillage) and maximum (during crop development) D_b on our site. Uncertainty on the WFPS estimation was around 16%. To follow its dynamics over the whole of 2012, WFPS was calculated with a mean D_b value equal to 1.25, while, during the campaign, from 10 May to 18 August, WFPS was calculated with a more realistic D_b value of 1.45.

The soil nitrate (NO_3^-) and ammonium (NH_4^+) contents were measured monthly from 2 April to 26 October. Nine soil samples were randomly collected from the top layer (0–30 cm), then frozen at −18 °C and analysed later for mineral nitrogen availability (N_{min}).

Vegetation dynamics was also monitored in terms of biomass production and green area index by collecting 20 plants five times during the growing season. At each date, dry matter production and green area were determined.

3. Results

3.1. Seasonal dynamics of N2O fluxes and of key drivers

3.1.1. Automated chamber flux data

Fig. 3 shows the mean N_2O flux dynamics per cycle of measurement ($F_{N2O\text{-}cycle}$) determined with the automated chambers during one year of monitoring. Over the campaign period, AC methodology led to a total number of 827 valid $F_{N2O\text{-}chamber}$ measurements against a possible total number of 2424 sampling periods over the whole campaign. Also, 66% of the data were filtered out following the quality check described in Section 2.2.2. On 404 theoretical means, there were 155 valid $F_{N2O\text{-}cycle}$.

N_2O emissions that did not present any diurnal dynamics but followed clear seasonal dynamics (Fig. 3) related to WFPS, soil temperature and mineral nitrogen availability dynamics. We could also identify periods with N_2O emissions of contrasting magnitude during the 100 days of campaign, which allowed us to evaluate the three methodologies together for three N_2O flux intensities: high, moderate and low (Table 2,). A large peak of N_2O emissions appeared consecutively to a

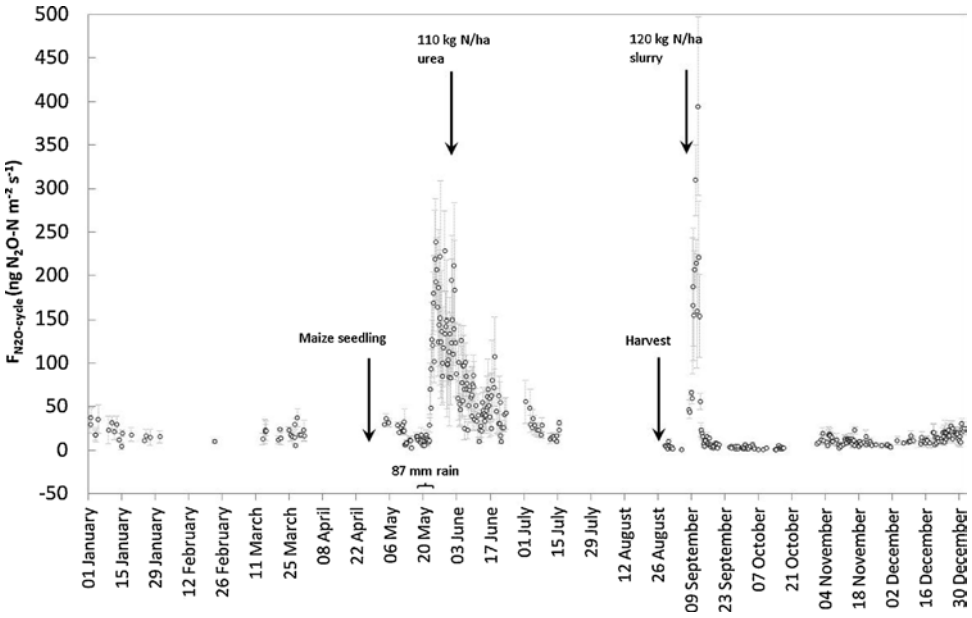

Fig. 3. Mean N_2O flux dynamics per cycle (every 6 h) from automated chambers, calculated for a number of chambers varying from 3 to 6. Error bars are $U_{FN2O\text{-}cycle}$. Main events and field operations are mentioned.

heavy rain event (87 mm in 4 days) between 19 and 22 May 2012 (Fig. 3), which increased WFPS from 46 ± 8% to more than 65 ± 11% (i.e. potentially 76%; Fig. 4). N_2O fluxes remained high from 22 May to 2 June, with mean N_2O emissions of 125.1 ± 8.9 ng N_2O-N m^{-2} s^{-1}. After the comparison period, the spreading of slurry on 7 September led to an immediate, very fleeting peak of N_2O emission, reaching a maximum of about 300 ng N_2O-N m^{-2} s^{-1} that lasted no more than six days. N_2O emissions of moderate magnitude, on average 57.2 ± 3.9 ng N_2O-N m^2 s^{-1}, were recorded from 3 to 20 June. Background emissions (low range), observed and calculated from 10 to 21 May and from 4 to 7 July achieved a mean value of 17.5 ± 1.6 ng N_2O-N m^{-2} s^{-1} (Table 2).

3.1.2. *Environmental conditions inside and outside the automated chambers*

Since maize was irrigated, WFPS inside and outside the automated chambers increased with both irrigation and rain events. WFPS frequently approached 60%, with a possible maximum error of ± 16.3% (depending on the bulk density values) because of the high clay content of the soil, which resulted in a very high water retention capacity. During the campaign, for which a bulk density of 1.45 was taken, mean values of 66.6 ± 4.2 inside the chambers and 56.3 ± 6.3% outside the chambers were recorded for both measurements for large range of N_2O fluxes, and mean values of 60.5 ± 7.6% and of 53.5 ± 9.4% were observed for the low range of N_2O fluxes inside and outside the automated chambers, respectively (Table 2). The two daily WFPS dynamics were comparable but highlighted the fact that soil outside the chamber dried slightly faster than soil inside the chamber (Fig. 4). Except between 10 and 21 May, values of T_{soil} (Fig. 5) outside the chambers always exceeded values of T_{soil} inside, with temperatures varying from 12.2 to 28.4 °C and from 13.4 to 24.7 °C, respectively, the minimum and maximum being observed on the same days (21 May and 28 June) for both. These results show that WFPS was higher and air temperature was lower inside than outside the automated chambers during the campaign and that a microclimate occurred.

3.1.3. *Seasonal dynamics of mineral nitrogen*

Nitrate and ammonium contents in the soil increased from January to June due to progressive organic matter mineralization in spring,

Table 1
Description of the three N_2O flux measuring set-ups that were compared during this field campaign: static and automated chamber systems and an eddy covariance set-up.

Aspect	Automated chambers	Static chambers	Eddy-covariance
Number of sample points	6 sample points	6 sample points	One sample point
Measurement type	Indirect: flux is calculated via the concentration increase over time during chamber closure	Indirect: flux is calculated via the concentration increase over time during chamber closure	Direct: flux is measured as the covariance of changes in turbulence and gas concentration
Sampling frequency	every 6 h (00:00, 06:00, 12:00 and 18:00)	4 dates : three times a day per position (May 11, May 24, June 6, July 1)	Half-hourly
Sampling area	0.161 m^2	0.12 m^2	Variable, maximum fetch of 300 metres
Principle	Automated chamber closure and continuous air sampling for 17 min in each chamber individually; Record of N_2O mixing ratio in the air coming from the chamber is recorded *in situ* every 10 s with a connected analyser.	Three chambers closed manually for 45 min; Air of the chamber is sampled with needle at 00, 15, 30, 45 min. N_2O concentration of the samples aremthen analysed *ex situ.*	Instantaneous *in situ* measurement of up and down motions including vertical wind component and mixing ratio of the gas of interest
Analyser	Low frequency infrared gas analyser (Thermofisher 46i, USA)	Gas Chromatograph and Mass Spectrometer (SRI 8610C, model 302)	High frequency Quantum Cascade Laser Spectrometer (GSMA product, France)

Table 2
Means and uncertainties (U_{range}) of N_2O emissions with EC (eddy covariance), AC (automated chamber) and SC (static chamber) methodologies for low, moderate and high ranges, and associated relative standard deviation (RSD), related to only temporal variation for EC measurements and to both spatial and temporal variations for chamber measurements; mean and standard deviation of soil temperature (T_{soil}) and of WPFS, calculated with a bulk density of 1.45, inside and outside the automated chambers (in °C and % respectively) for each range. N is the number of values, equivalent to the total number of $F_{N2O\text{-}chamber}$ for AC and SC methodologies, and to the total of half-hourly fluxes for EC methodology.

		^{F}N2O-EC ng N_2O-N/m^2/s	^{F}N2O-AC ng N_2O-N/m^2/s	^{F}N2O-SC ng N_2O-N/m^2/s	^{WFPS}inside %	^{T}soil-inside °C	^{WFPS}outside %	^{T}soil-outside °C
Low Range (10–21 May)	Mean	15.7	17.5	14.7	60.5	19.1	53.5	19.6
	$^{U\ range\ ,\ SD}$	*10.1*	*1.6*	*2.2*	7.6	3.6	9.4	4.2
	RSD	151%	71%	26%				
	N	87	69	11	69	69	150	150
	Min	−52.2	5.6	10.8	55.1	11.7	44.8	11.3
	Max	62.2	55.7	18.6	77.6	23.4	74.9	26.5
Moderate range (3–20 June)	Mean	33.8	57.2	41.6	62.0	21.0	50.7	22.6
	$^{U\ range\ ,\ SD}$	*3.9*	*3.9*	*6.6*	2.3	3.2	3.5	4.9
	RSD	58%	47%	13%				
	N	139	137	18	137	137	222	222
	Min	8.9	23.0	35.6	58.5	15.0	46.2	14.7
	Max	84.2	129.6	46.0	68.8	27.3	60.3	34.6
High range (22 May -2 June)	Mean	125.3	125.1	131.7	66.6	22.4	56.3	24.5
	$^{U\ range\ ,\ SD}$	*8.0*	*8.9*	*22.1*	4.2	4.9	6.3	6.4
	RSD	35%	30%	23%				
	N	85	114	17	114	114	156	156
	Min	70.1	49.2	112.2	59.9	14.0	47.1	13.6
	Max	259.4	207.7	166.7	73.9	30.5	68.7	35.3

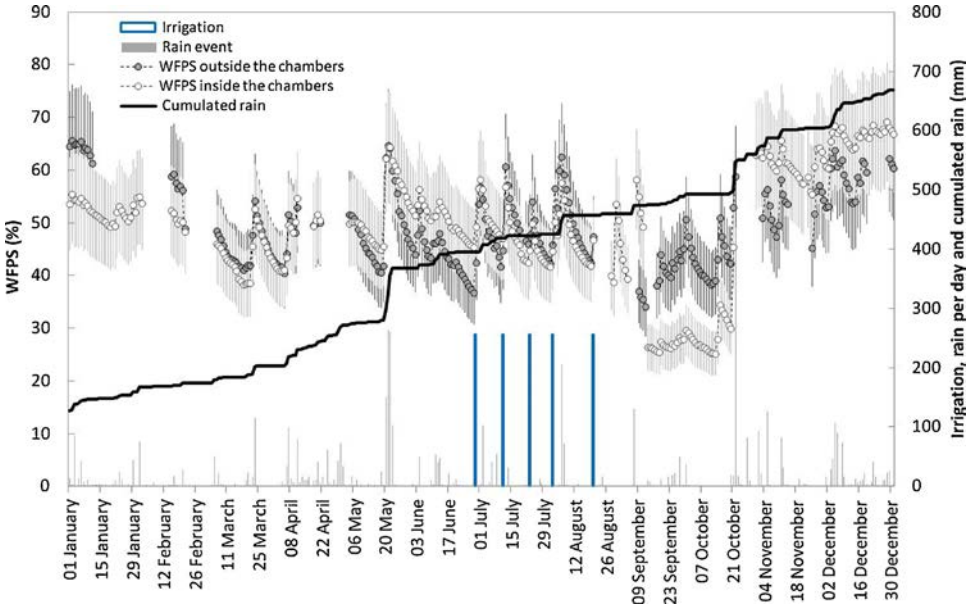

Fig. 4. Daily average dynamics of water filled pore space calculated with a mean bulk density (D_b) value equal to 1.25 inside (white circles) and outside (grey circles) the automated chambers, cumulated (black line) and daily precipitation (grey bars), irrigation events (blue bars). Error bars for WFPS are ± 16.3% of the mean value, reflecting the uncertainty due to the D_b value chosen. (For interpretation of the references to color in this figure legend, the reader is referred to the web version of this article.)

reaching 123 and then 285 kg N.ha^{-1} after the spreading of the equivalent of 110 kg N.ha^{-1} urea. A progressive decrease in soil N content was then observed concomitantly with the increase in the maize biomass produced. Then nitrate and ammonium contents in the soil increased following the application of 120 kg N ha^{-1} as slurry (Fig. 6).

3.2. Flux data from chamber methodologies

Over the campaign period, SC methodology led to a total number of 54 valid $F_{N2O\text{-}chamber}$ measurements against a possible total number of 65 sampling periods over the whole campaign. Only 17% of the data were filtered out. We also could calculate 12 valid SC $F_{N2O\text{-}cycle}$. Despite the limited number of measurement dates, results obtained from the SC methodology successfully captured the main N_2O emission events (Fig. 7) and the range recorded using the automated chambers, with a mean of 14.7 ± 2.2 and of 131.7 ± 22.1 ng N_2O-N m^{-2} s^{-1} in the lowest and highest ranges, respectively (Table 2). In the intermediate range, SC recorded a mean N_2O flux value significantly lower than that recorded with AC: 41.6 ± 6.6 versus 57.2 ± 3.9 ng N_2O-N m^{-2} s^{-1} (Fig. 7).

Whatever the chamber system, the absolute random uncertainty was higher for high N_2O fluxes and inversely lower for low N_2O fluxes (Fig. 8). Absolute random uncertainties never exceeded the mean value of fluxes whatever the flux range.

3.3. Spatial and temporal variabilities of N_2O fluxes

Static chambers – Daily F_{N2O} followed the same dynamics but with different magnitudes (Table 3), from very low (chamber 6) to very high (chamber 1). The absolute random uncertainties and RSD coefficient calculated per chamber for a given day showed that the diurnal variability was particularly strong during the N_2O peak on 24 May, illustrating the strong impact of T_{soil} when N_{min} (around 75 kg N ha^{-1}) and WFPS (66.6 ± 4.2%) were in favour of N_2O production. On that

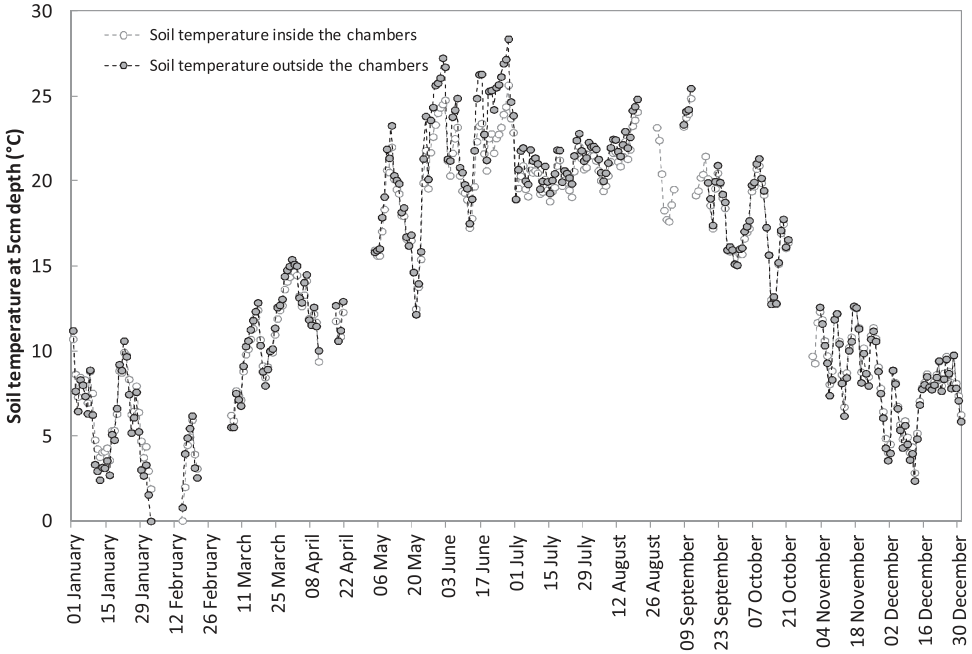

Fig. 5. Daily dynamics of soil temperature at 5 cm depth inside (white circles) and outside (grey circles) the automated chambers.

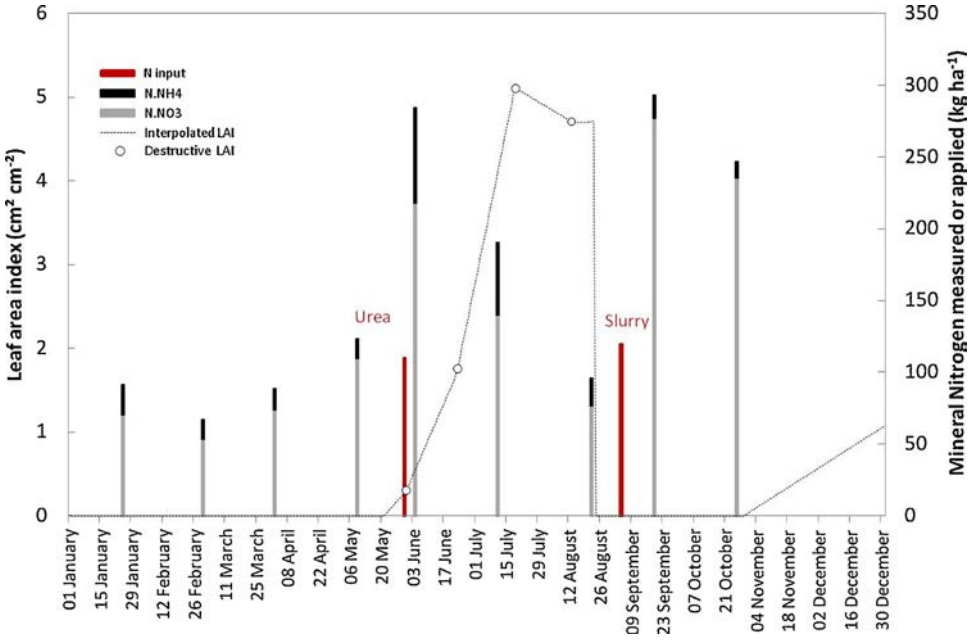

Fig. 6. Daily leaf area index dynamics of maize, soil mineral nitrogen content dynamics in the upper layer (0–30 cm, grey and black bars) and mineral nitrogen input (red bars) during 2012. (For interpretation of the references to color in this figure legend, the reader is referred to the web version of this article.)

day, T_{soil} varied from 15 °C at daybreak to 27.5 °C at noon and N_2O fluxes varied according to T_{soil} dynamics (data not shown). The spatial relative standard deviation (RSD_{spat}), always higher than 30% and up to 62% on 6 June (Table 3), also illustrated the high spatial variability of N_2O fluxes whatever the range of F_{N2O}. The mean daily flux could vary from 38.7 ± 5.2 to 230.5 ± 11.3 ng N_2O-N m^{-2} s^{-1} for chambers 6 and 2, respectively, during the highest emissions and from 3.3 ± 0.7 to 7.7 ± 1.0 ng N_2O-N m^{-2} s^{-1} for chambers 1 and 6, respectively, during the lowest emissions.

Automated chambers - The daily dynamics of N_2O fluxes and of WFPS in each automated chamber over the campaign (Fig. 9) revealed similar N_2O flux dynamics between chambers but with large differences in magnitude as observed for static chambers, from very low (Chamber 5) to very high (Chamber 2) N_2O emissions. The maximum emissions occurred at the same time, between 24 and 27 May, for all chambers and ranged from 61.7 ± 15.2 (chamber 5) to 299.3 ± 81.7 ng N_2O-N m^{-2} s^{-1} (chamber 1). Overall, chambers 1, 2 and 4 showed the highest mean daily N_2O emissions. The daily dynamics of WFPS evolved similarly among the chambers but with different levels from the beginning of the campaign: from 50% for chamber 3 to around 70% for chamber 1 (Fig. 9). Chambers 1 and 2 also had the highest WFPS, whereas chamber 4 presented a WFPS equivalent to that of the others. The value on 21 May was one of the strongest WFPS measured: from 69% for chamber 3 to 84% for chamber 1.

The RSD coefficient for AC varied from 71% to 30% (Table 2). It decreased with increasing F_{N2O} range, highlighting lower and higher

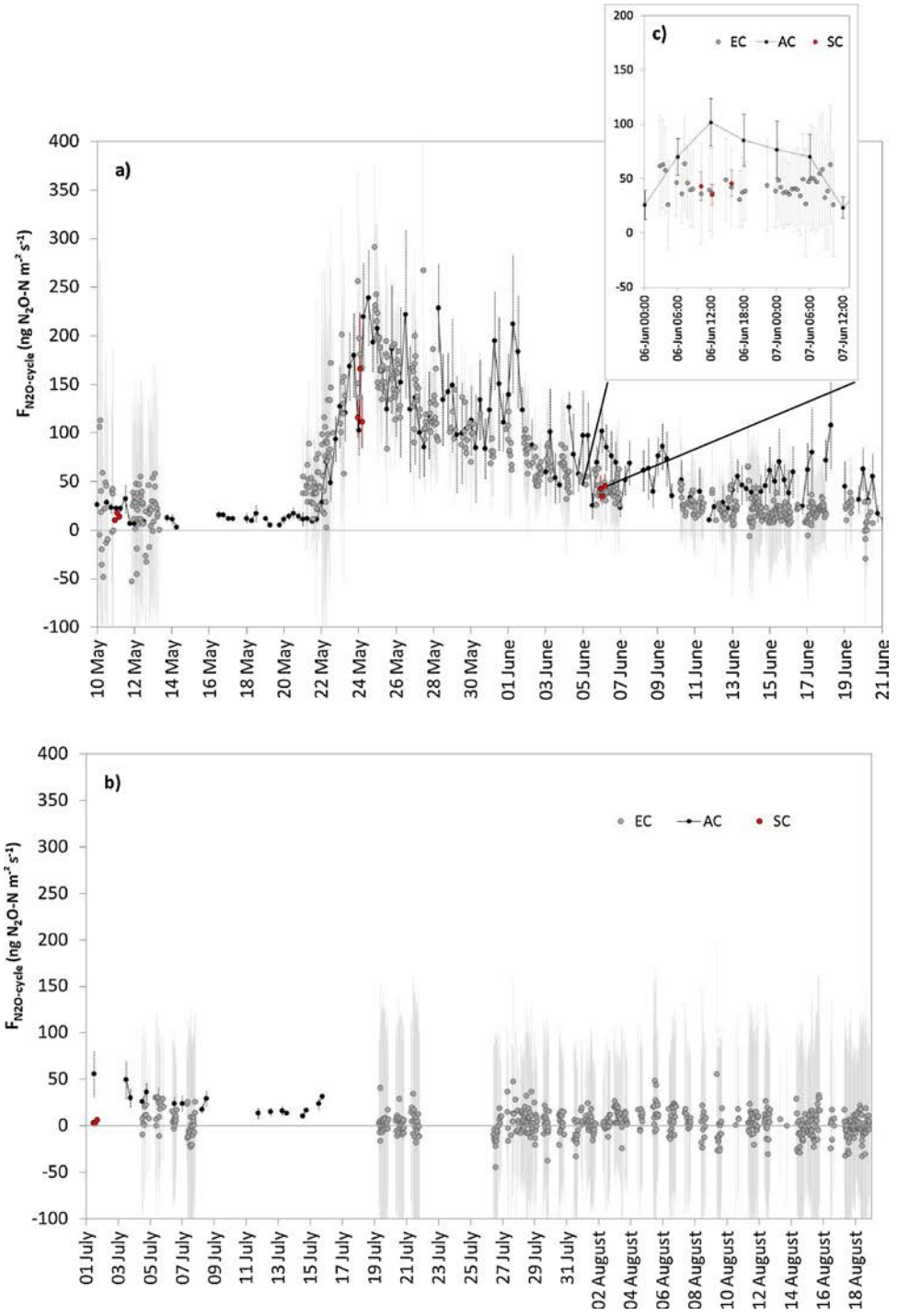

Fig. 7. Dynamics of N_2O fluxes at a half-hourly time step for EC method and per cycle ($F_{N2O\text{-}cycle}$) for both AC and SC methods with associated error U_{EC} and $U_{F2O\text{-}cycle}$ for EC and chamber methods respectively. a) period between 10/05/2012 & 21/06/2012; b) period between 01/07/2012 & 18/08/2012; c) zoom on the period between 06/07/2012 & 07/07/2012. (For interpretation of the references to color in this figure legend, the reader is referred to the web version of this article.)

spatial and temporal variability of F_{N2O} for high and low emissions respectively.

3.4. N_2O fluxes from eddy covariance methodology

A total of 1196 valid half-hourly EC fluxes (corresponding to data coverage of 51%) were obtained from the initial 2350 measurements. The filtering procedures eliminated 4, 19, 9 and 20% of the initial data set on quality flag, U*, Webb and footprint criteria, respectively. As the dry mixing ratio was not measured directly, we investigated the effect of the water vapour on the fluxes.

3.4.1. Water vapour effects

To investigate the possible interference effect of water vapour on N_2O fluxes, dilution and/or cross-sensitivity of the laser data of the period from 1st July to 18 August 2012 were chosen, which had small N_2O fluxes, recorded with a static chamber (< 4.6 ng N_2O-N m^{-2} s^{-1}, below the detection limit of EC methodology). The more water vapour there was inside the cell, the lower was the N_2O molar fraction (Fig. 10). The F_{N2O} measured and calculated with the EC system,

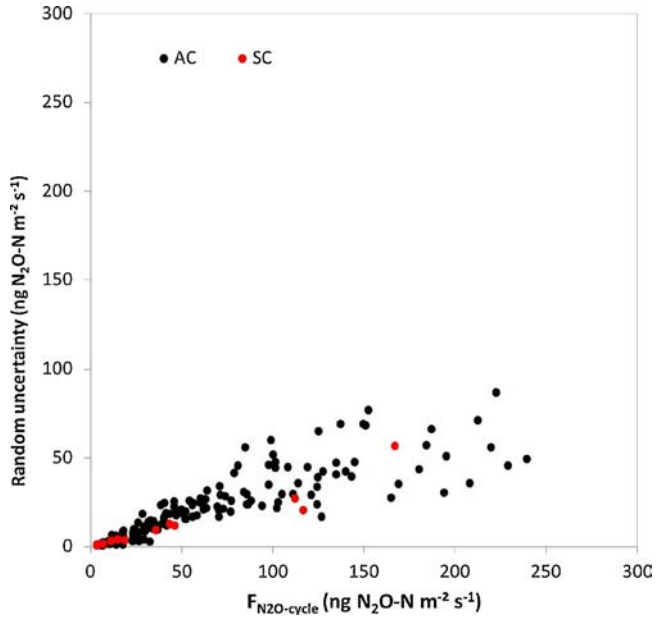

Fig. 8. Relation between mean $F_{N2O\text{-}cycle}$ and associated random uncertainty related to spatial variability (U_{sv}) according to the AC (black circles) and SC (red circles) methodologies. (For interpretation of the references to color in this figure legend, the reader is referred to the web version of this article.)

without any dilution effect correction, also clearly showed a diurnal, negative correlation with water vapour fluxes inside the cell (Figs. 10 and 11). When the water vapour dilution effect correction was applied, even if the scatter plot showed a worse distribution ($R^2 = 0.1$ versus $R^2 = 0.8$), the negative correlation was reduced by about 80% according to the slope values (Fig. 11). A negative correlation and negative fluxes still remained.

3.4.2. EC flux uncertainties

Absolute and relative systematic uncertainties were calculated for each half-hourly EC flux (Fig. 12). Absolute systematic uncertainties varied between 25 and 180 ng N_2O-N m^{-2} s^{-1} for F_{N2O} ranging from -52.2 to 291.7 ng N_2O-N m^{-2} s^{-1}. The relative systematic uncertainties showed a lognormal distribution. The lower the EC N_2O fluxes were, the higher the relative systematic uncertainties were. U_{op} rose with increasing standard deviation of N_2O molar fraction and U_{webb} rose with increasing LE fluxes (Fig. 13). The propagated absolute systematic uncertainties were 10.1, 3.9 and 8.0 ng N_2O-N m^{-2} s^{-1} for the low, moderate and high ranges of EC N_2O fluxes, respectively (Table 2).

3.4.3. Comparison of N2O fluxes between chamber and eddy covariance methodologies

EC measurements showed N_2O flux dynamics similar to those measured with the automated and static chambers (Fig. 7). EC measurements showed moderate to high N_2O fluxes during the spring period following rain, irrigation and nitrogen fertilization events (Fig. 7). Very low N_2O fluxes were mainly recorded during the summer period, with high temporal variability as demonstrated in Fig. 7 and with an RSD coefficient of 151% on the period 10–21 may (Table 2). As with the chamber methods, the largest N_2O flux was obtained after the rain event of 87 mm between 19 and 22 May, reaching 291.7 ± 82.9 ng N_2O-N m^{-2} s^{-1}. In a comparison with SC and AC methodologies, for a mean moderate EC flux of 33.8 ± 3.9 ng N_2O-N/m^{-2}/s, EC measurements showed poor agreement with the N_2O fluxes measured by means of the automated chambers (57.2 ± 3.9 ng N_2O-N m^{-2} s^{-1}). Low and high EC N_2O emissions agreed better with the fluxes measured with the automated chambers (Table 2).

Consecutively to filter out procedure, concomitant EC and AC or SC

Table 3
Mean daily N_2O fluxes measured in the six static chambers (SC) in ng N_2O-N/m^2/s, temporal and spatial relative standard deviation (RSD_{temp} and RSD_{spat}) for each date of measurement.

Date	SC 1			SC 2			SC 3			SC 4			SC 5			SC 6			All chambers
	mean	^{U}day	RSD_{temp}	mean	^{U}day	RSD_{temp}	mean	^{U}day	RSD_{temp}	mean	^{U}day	RSD_{temp}	mean	^{U}day	RSD_{temp}	mean	^{U}day	^{RSD}temp	^{RSD}spat
11-May	N/A	N/A	N/A	N/A	N/A	N/A	15.9	± 2.3	30%	21.9	± 2.7	29%	10.8	± 2.7	60%	N/A	N/A	N/A	56%
24-May	179.7	± 11.1	59%	230.5	± 11.3	48%	156.1	± 8.9	44%	102.5	± 7.1	42%	58.4	± 4.0	24%	38.7	± 5.2	59%	58%
6-Jun	71.2	± 4.7	26%	62.8	± 3.2	14%	19.8	± 1.8	14%	36	± 2.5	15%	26.1	± 4.2	59%	12.9	± 1.9	25%	62%
1-Jul	3.3	± 1.1	31%	N/A	N/A	N/A	N/A	N/A	N/A	5	± 2.3	88%	2.6	± 1.3	54%	7.7	± 1.3	18%	43%

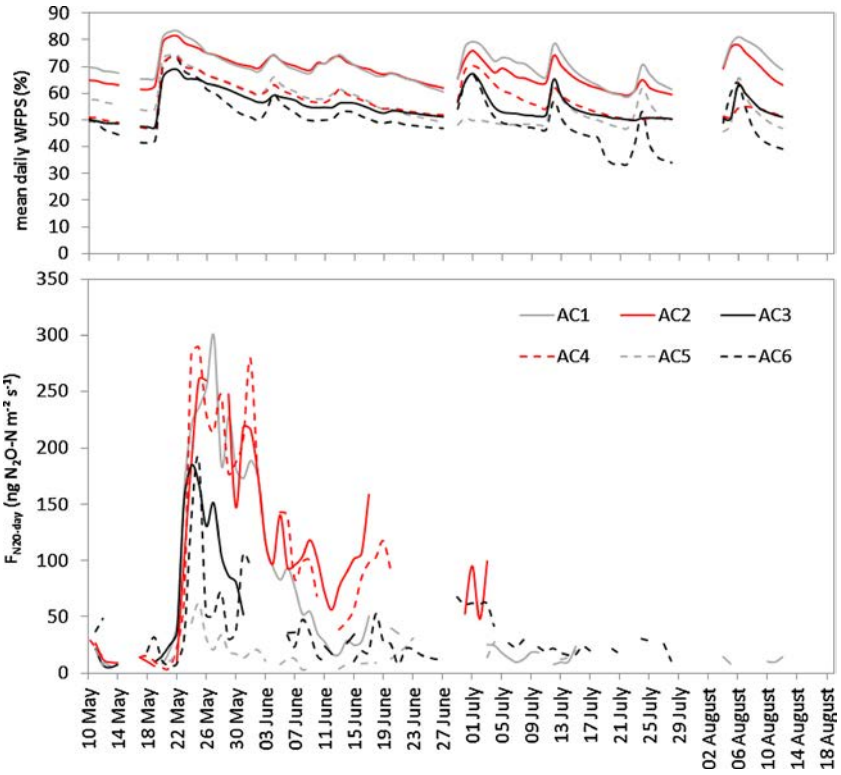

Fig. 9. Daily dynamics of F_{N2O} in each automated chamber and associated WFPS over the comparison campaign. (For interpretation of the references to color in this figure legend, the reader is referred to the web version of this article.)

measurements were unfortunately not numerous (91 for AC and only 5 for SC, considering $F_{N2O\text{-}cycle}$). However, the comparison showed good correlation between the methodologies (Fig. 14, $R^2 = 0.6368$).

4. Discussion

4.1. Magnitude of N_2O fluxes over an irrigated maize field

So far, few long campaigns of N_2O flux measurements have been carried out over croplands (Pattey et al., 2007; Desjardins et al., 2010, Reinsch et al., 2018) and most of such measurements have been based on the use of chambers or gradient methods (Pattey et al., 2006; Denmead et al., 2010, Yuhui et al., 2017, Reinsch et al., 2018; Kostyanovsky et al., 2018). Laville et al. (1999) measured N_2O emissions with both static chambers and micrometeorological methods (eddy covariance and flux-gradient) over irrigated and fertilized maize fields. After the input of 200 kg N ha^{-1} into the soil, they measured N_2O fluxes ranging from 20 ng N_2O-N m^{-2} s^{-1} to 400 ng N_2O-N m^{-2} s^{-1} with the micro-meteorological methodologies and from 25 to 275 ng N_2O-N m^{-2} s^{-1} with the static chambers. In the present work, equivalent ranges of fluxes from 15.7, 17.5 and 14.7 to 125.3, 125.1 and 131.7 ng N_2O-N m^{-2} s^{-1} were recorded with the automated chamber, static

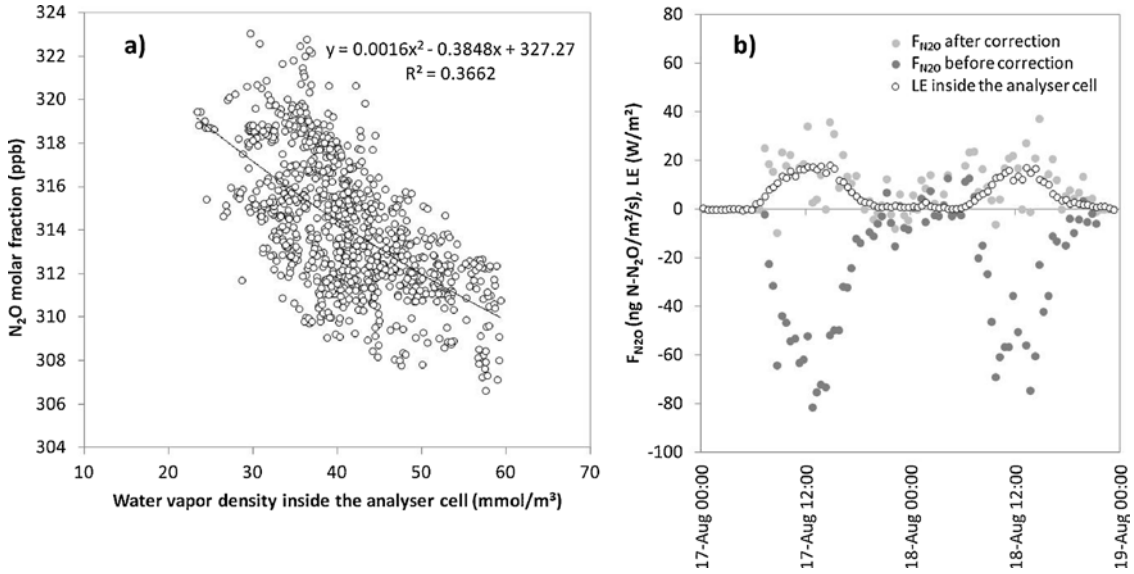

Fig. 10. a) N_2O molar fraction versus water vapour density for situation with fluxes recorded below 60 ng N_2O-N m^{-2} s^{-1}; **b)** Half-hourly dynamics of N_2O fluxes versus latent heat fluxes (simulated inside the cell) during two days of low N_2O fluxes.

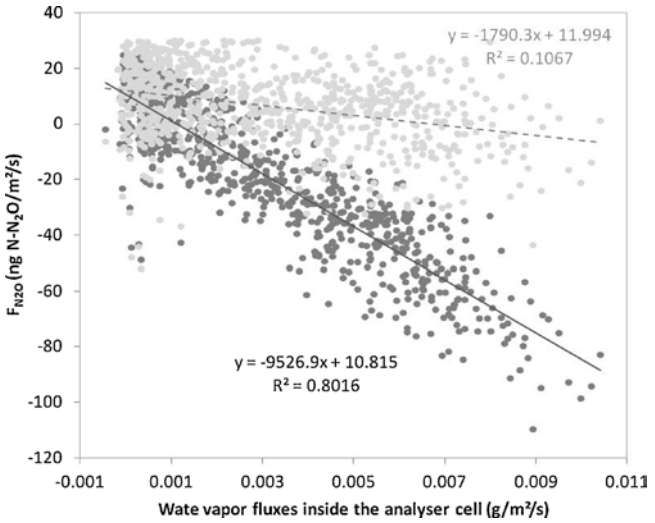

Fig. 11. Half-hourly N_2O fluxes versus water vapour fluxes from 1 July to 18 August 2012. Light grey circles: no density correction, dark grey circles: with only WPL correction applied. The solid lines indicate the results of least-squares linear regressions for both datasets.

chamber, and EC methodologies respectively. N_2O emission peaks occurred with strong increases of WFPS, following rain or slurry spreading events, or were associated with favourable N_{min} availability coming from spring mineralization of the previously incorporated solid manure or from mineral or organic fertilization. Such short-lived increases in N_2O emissions occurred twice during the field campaign but with different durations. The fluxes reached lower magnitudes at the end of May and then slowly faded away to background level in around 20 days over young maize, in wet soil conditions. Nevertheless, following slurry spreading in September, the emission was strong and short: the flux intensities decreased rapidly (over about 6 days) with drier soil conditions. Similar short-lived N_2O emissions have been reported in other studies (Clayton et al., 1997; Leahy et al., 2004, and Jones et al., 2011). Despite the positive effect of irrigation on the WFPS between mid-July and mid-August, $F_{N2O\text{-}cycle}$ remained mostly lower than during May, probably because of reduced N_{min} availability combined with lower T_{soil}. Minimum and maximum values of WFPS observed in the high range of N_2O emissions corresponded to the optimal range of WFPS found in the literature for N_2O production (Bateman and Baggs, 2005). Moderate and lower $F_{N2O\text{-}cycle}$ corresponded to lower mean WFPS, T_{soil}, and N_{min} availability. However, in this paper, we focus on an intercomparison of the methodologies, without aiming to explain their differences by further investigation of the process involved or to quantify the role of large range biotic and abiotic factors in the nitrification-denitrification processes.

4.2. Comparison of methodologies

4.2.1. Turbulence effects

Despite the strong difference in measurement scales, i.e. from the square metre to footprint scale in spatial sampling, and sampling frequencies varying from one-off measurements for manual chambers to continuous measurement with EC, the three methodologies agreed well when capturing the temporal dynamics and magnitude of N_2O fluxes at "fine" timescale from the cycle measurement time step, especially when F_{N2O} were strong, in the first period of the campaign. In comparison, Laville et al. (1999) observed marked discrepancies between their 30 closed static chambers and two micrometeorological methodologies when considering hourly measurements. Their results were improved when fluxes were integrated over 10 days and averaged over all the chambers. We also averaged the flux calculated from the 6 SC and 6 AC chambers. Nevertheless, while the SC and EC methodologies still agreed for moderate fluxes, the AC measurements differed considerably from both SC and EC measurements. This is particularly well illustrated in Fig. 7c for 6 and 7 June. The AC methodology gave a higher estimation of mean N_2O emissions. The same apparent overestimations were observed from 13 to 18 June between EC and AC methodologies and on 1 July between SC and AC methodologies. It should be noted that the strongest divergences were recorded when the aerodynamic conditions inside the vegetation were characterized by low turbulence. Those periods of divergences between methodologies matched with a well developed and tall vegetation. A tall vegetation inevitably attenuated or even cancelled the turbulence between the top of canopy and the soil surface. As reported in the material and methods section, the design of the AC was different from that of the SC. The walls of the AC (22.7 cm high) were permanently inserted in the ground, unlike the SC ones. Only the lid was movable in the automated chamber. This design, associated with the high molar mass of N_2O, could cause storage of N_2O inside the chamber during periods when no measurements were recorded. This accumulation could modify the diffusion gradients from soil porosity to the atmosphere. When the chamber was closed, the fan was triggered to ensure homogeneity of the air in the chamber. It remained active throughout the recording period. The aerodynamic conditions were then modified inside the chamber during the whole measurement period. The high turbulence in the chamber induced a decrease of the thickness of the boundary layer at the soil surface. This reduction of the boundary layer compared to the external conditions (i.e. periods characterized by low turbulence) caused preferential paths of gas diffusion towards the inside of the chamber. Thus the cumulative effect of changing aerodynamic conditions in the chamber due to the use of the fan, associated with pre-storage of N_2O prior to the measurement period, may explain the overestimation of the flux compared to the EC and SC data in low turbulence conditions. This process has already been described in comparative studies of soil respiration measurement systems using chambers (Le Dantec et al., 1999; Ngao et al., 2006; Christiansen et al., 2011; Rochette and Eriksen-Hamel, 2008; Rochette and Hutchinson, 2005). For the method of static chambers in particular, previous works have shown that the absence of air mixing in the upper part of the chamber before and during the measurement causes a severe underestimation, up to 36% in some cases (Liu and Si, 2009; Christiansen et al., 2011; Pihlatie et al., 2013). All these studies demonstrated the strong impact of the type and intensity of air mixing in the measurement chamber on the quantification of the soil CO_2 or CH_4 flux. Moreover, these differences in aerodynamic conditions between the outside and the inside of the chamber could also cause a pressure difference, especially during windy periods. It was previously reported that an overpressure or a depression, even a very weak one, strongly affected the measurement of a gaseous flow at the surface of the ground (Bain et al., 2005; Davidson et al., 2002; Hutchinson and Livingston, 2001; Hutchinson and Mosier, 1981; Xu et al., 2006).

The main advantage of the EC method is that it is not intrusive and that it avoids soil and airflow disturbances in the sampling area. However, one of its limits is that some criteria concerning micro-meteorological conditions have to be met for the measurement to be valid (high turbulence, no advection…). In this study, 50% of the data were filtered out, mainly using criteria such as footprint area and low friction velocity during night-time. Data filtering is an important issue, especially for annual budget calculations.

4.2.2. Water vapour effects

For the background N_2O flux range, even though the EC methodology gave satisfactory values on average, the data remained highly variable in time with very large dispersion around the mean (range or per cycle) and large random uncertainties, mainly due to the Webb correction. During the campaign, the QCLAS sensor did not measure N_2O and the water vapour fluctuation at the same time and place (inside the analyser cell) so did not provide the dry mixing ratio of N_2O directly. Moreover, the potential cross-sensitivity of the QCLAS to water

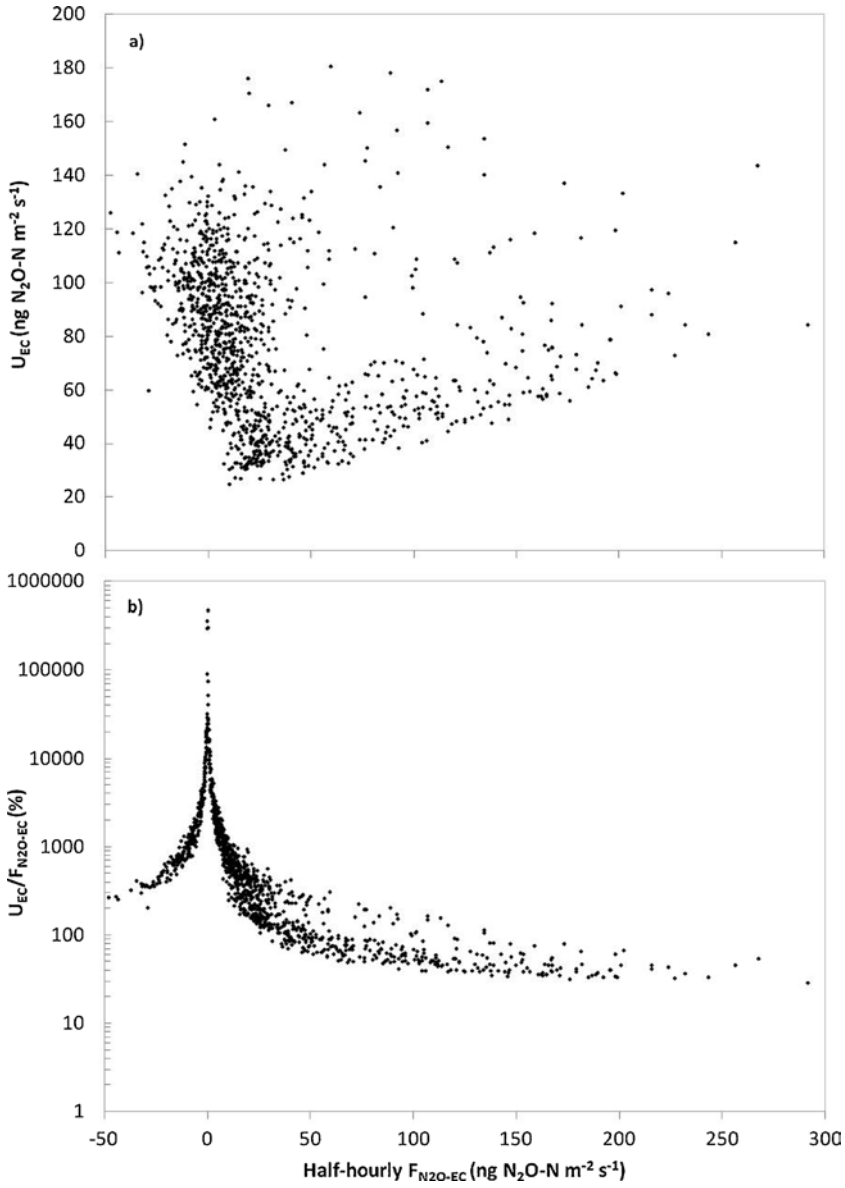

Fig. 12. a) Absolute and b) relative systematic uncertainties of half-hourly EC N_2O fluxes as a function of mean half-hourly EC N_2O fluxes.

vapour was unfortunately not quantified as recommended in Neftel et al. (2010). In this study, the EC methodology recorded N_2O fluxes varying from -52.2 ± 88.1 to 89.4 ± 63.0 ng N_2O-N m^{-2} s^{-1}. Individual measurements with large negative but not persistent values, as observed at the beginning of the campaign, may have been due to random errors of the measurement system. However, persistent measurements with large negative values, as observed during summer, must be considered with special care. They may have resulted from a poor estimation of the Webb term (Aubinet et al., 2012) and/or from a failure to correct for the cross-sensitivity effect. Neftel et al. (2010), in following a conservative upper limit approach, postulated that persistent N_2O uptake above 16.8 ng N_2O-N m^{-2} s^{-1} was unrealistic. The occurrence of a possible systematic error due to the omission of cross-sensitivity correction in that study could explain the observed and unexpected persistent negative fluxes during summer where water vapour fluxes were high (data not shown).

The half-hourly EC fluxes showed systematic uncertainties during most of the campaign that, although high and variable, were similar to those calculated in Kroon et al. (2010), where absolute systematic uncertainties ranged from 20 to 400 ng N_2O-N m^{-2} s^{-1} for a F_{N2O} range of 0 to 750 ng N_2O-N m^{-2} s^{-1}. When the contribution of each term to the total uncertainty was investigated, the high systematic uncertainties were found to be mainly due to the Webb term during the second period of the campaign, in August, when low N_2O fluxes and a strong effect of water vapour were observed. Accordingly, the Webb term calculated to correct N_2O fluxes, and the resulting systematic uncertainties, were large. This underlined the need to dry the air sample or measure the water vapour fluctuation directly inside the analyser cell. However, applying only the Webb correction was not sufficient to counteract the negative dependency of N_2O fluxes on water vapour fluxes, and negative fluxes remained. Beyond the physical point of view, Nicolini et al. (2013), in their literature overview of micrometeorological N_2O flux measurements, pointed out that several cases of negative fluxes had been reported on different terrestrial ecosystems, such as grassland, peatland and cropland (Neftel et al., 2007, 2010; Flechard et al., 2005; Jones et al., 2011). At such sites, high organic matter content coupled with favourable WFPS (very low oxygen level) might have led to a complete denitrification reaction, i.e. the reduction of N_2O to the final product, N_2 (Neftel et al., 2007). In the present study, none of these assumptions was verified and the quality control criteria we used did not help to reject or explain the negative fluxes.

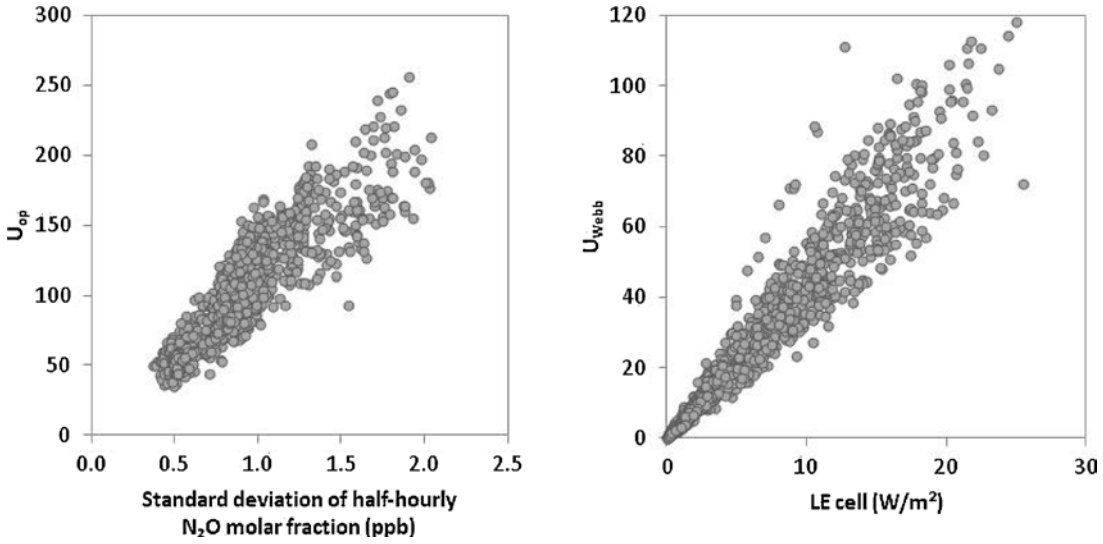

Fig. 13. Half-hourly one sampling-point (U_{op}) and Webb (U_{Webb}) uncertainties versus mean half-hourly standard deviation of N_2O molar fraction and of mean latent heat fluxes (LE), respectively, inside the analyser cell.

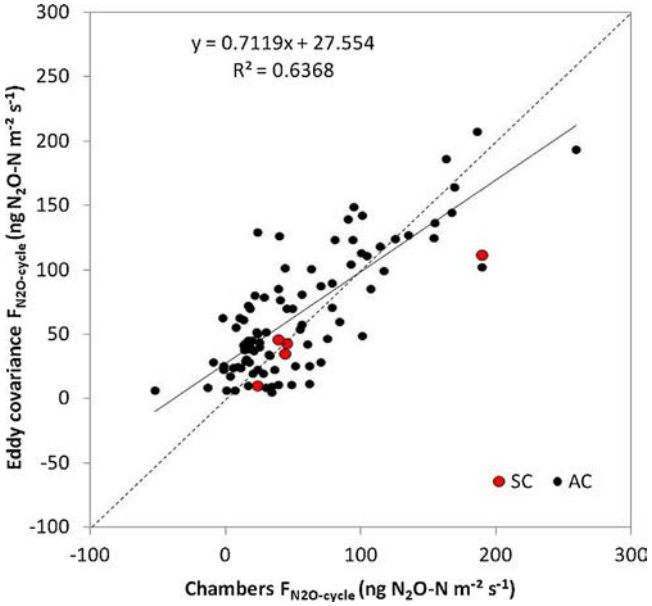

Fig. 14. Comparison of synchronized mean Eddy covariance $F_{N2O\text{-}cycle}$ with mean automated and static chambers $F_{N2O\text{-}cycle}$. (For interpretation of the references to color in this figure legend, the reader is referred to the web version of this article.)

4.3. Spatial and temporal variabilities

For many years, set-ups based on static or automated chambers have been widely used to monitor N_2O flux dynamics, mainly because they are relatively cost effective and easy to use (Denmead et al., 2008; Rochette and Eriksen-Hamel, 2008). N_2O fluxes measured using both chamber methodologies and their associated RSD coefficients highlighted the high spatial variability from the lowest to the highest range of fluxes, as Laville et al. (1999) had already observed in their study using 30 static chambers. Our results confirmed the presence of spatial hotspots of N_2O emissions inside the footprint of the EC system, driven either by hotspots of organic matter or N_{min} or by microclimates with higher or lower values of WFPS and T_{soil}.

Although the spatial representativeness of chamber methodologies should be further investigated in comparison with the EC measurements according to the wind direction and footprint area, our results proved that a set of 6 automated or static chambers distributed through the EC footprint area were sufficient to integrate spatial heterogeneity at our site and to capture the mean daily N_2O flux dynamics well. In addition, the sampling frequency (every 6 h for each chamber, i.e. a total of 24 measurements per day) for the automated chambers allowed us to reproduce the mean daily emission averages found by the EC methodology. For the static chambers, the diurnal sampling frequency (every 3 h, i.e. 18 measurements per day) was conclusive for a given date with small divergences, probably resulting from varying soil conditions within the sampled area. However, the sampling frequency (only 4 days during the whole campaign) was not sufficient to capture all the main N_2O emission events and variations, and demonstrates the need for considerable manpower with this method. Thus SC are not easily deployable for long periods and/or for night-time measurements. Measurements are performed according to a fixed schedule, ideally at the end of winter, several times during the three weeks after a fertilization event, etc. It is then crucial to anticipate the potential period of significant N_2O emissions so as to catch the dynamics of N_2O fluxes for a given type of management.

The EC methodology has the advantage of integrating spatial heterogeneity and monitoring the temporal dynamics of N_2O fluxes well. The high frequency and large scale of EC measurement allowed most of the N_2O flux events to be captured. This is a very important advantage when the aim is to assess an accurate annual GHG budget and to make a finer analysis of which processes trigger N_2O emissions. However, the high systematic uncertainties observed during the first period of the campaign, especially in May when F_{N2O} was high, were mainly due to the one point sampling term. The one point sampling term in the systematic uncertainty calculation depended strongly on the standard deviation of the N_2O molar fraction. Moreover, the higher the mean N_2O molar fraction values were, the higher were their associated standard deviations (data not shown) and, thus, the calculated systematic uncertainty. This analysis revealed that, even if a QCLAS is designed for very precise, fast measurement of N_2O fluctuations, the latter remain large and difficult to capture.

5. Conclusion

In the context of climate change, international infrastructures like NEON (National Ecological Observatory Network) or ICOS (Integrated Carbon Observation System) are implemented to monitor long-term GHG emissions and to better characterize emissions and their proxies at large scale. With the underlying objective of joining such international

frameworks, we conducted an inter-comparison campaign of N_2O flux measurement methodologies with static/automated chambers and the eddy covariance method to evaluate the constraints, limits and advantages of each system, and their representativeness, accuracy and complementarities.

In agro-ecosystems with unlimited amounts of nitrogen available, such as fertilized crops with potentially significant and high N_2O fluxes, the EC methodology proved to be a promising way to more accurately evaluate the real contribution of N_2O emissions in the whole agro-ecosystem GHG budget in the long term, and to identify the potential levers to attenuate it. Thanks to its higher sampling frequency, the EC methodology should be a useful method to better evaluate the effect of varying environmental factors on N_2O fluxes and to improve the formalism used in existing models intended to reproduce and predict them. Research on N_2O flux measurement with the EC method is still in progress to assess the robustness of the method. Including the measurement of the water vapour component directly inside the analysis cell will help to strongly reduce systematic uncertainties linked to this correction. Research with the use of chambers is needed to perform soil process studies and characterize the high spatial variability occurring in plot functioning (so called "hotspots") as observed in our study. An understanding at "hotspot" scales may improve knowledge of the observed process at macroscale (field level). They can also be used in larger scale meteorological conditions (Rochette and McGinn, 2004) than the EC methodology. However, chamber methods, whether static or automated, still need improvement to avoid physical disturbances (turbulence, pressure). In addition, on crop sites, crop management imposes strong constraints on installing and removing the set of chambers. Potential failure to detect hot-moments could also result from the low sampling frequency. Even with the best organization and intense deployment, this method is not the most suitable for calculating an annual budget. Nevertheless, static chambers remain a commonly used method because they are cheap and easy to operate in situ, although this ease of operation is offset by the time spent in the laboratory for the sample analyses. Thus there are several factors in favour of one or the other methodology, depending on the spatial/temporal variability, magnitude of uncertainties, field constraints and scientific objectives but, to date, the methodologies remain complementary.

Acknowledgements

We wish to thank the anonymous reviewers for their valuable comments, which greatly helped us to improve the paper. Observational data were collected at the Regional Spatial Observatory (OSR) and supported by funding from ICOS-France. OSR facilities and staff are funded and supported by the Midi-Pyrenees Observatory (OMP), Paul Sabatier University of Toulouse, CNRS (Centre National de la Recherche Scientifique), CNES (Centre National d'Etudes Spatiales) and IRD (Institut de Recherche pour le Développement). This campaign was specifically supported by OMP via a BQR grant. We also acknowledge Pascal Keravec, Hervé Gibrin, Bernard Marciel and Raphael Noual for their valuable help in the field and their technical support. We are grateful to Jerôme Cros who helped with data processing.

References

Bain, W.G., Hutrya, L., Patterson, D.C., Bright, A.V., Daube, B.C., Munger, J.W., Wofsy, S.C., 2005. Wind-induced error in the measurement of soil respiration using closed dynamic chambers. Agric. For. Meteorol. 131, 225–232.

Baldocchi, D., 2014. Measuring fluxes of trace gases and energy between ecosystems and the atmosphere - the state and future of the eddy covariance method. Glob. Chang. Biol. 20, 3600–3609.

Barton, L., Wolf, B., Rowlings, D., Scheer, C., Kiese, R., Grace, P., Stefanova, K., Butterbach-Bahl, K., 2015. Sampling frequency affects estimates of annual nitrous oxide fluxes. Sci. Rep. 5, 15912.

Bateman, E., Baggs, E., 2005. Contributions of nitrification and denitrification to N2O emissions from soils at different water-filled pore space. Biol. Fert. Soils 41, 379–388.

Bessou, C., et al., 2010. Modelling soil compaction impacts on nitrous oxide emissions in arable fields. Eur. J. Soil Sci. 61 (3), 348–363.

Beziat, P., Ceschia, E., Dedieu, G., 2009. Carbon balance of a three crop succession over two cropland sites in South West France. Agric. For. Meteorol. 149 (10), 1628–1645.

Bureau, J., 2017. Nitrous Oxide Emissions by Agricultural Soils: Effect of Temperature Dynamics; Up-Scaling Measurements From the Plot to the Landscape. Earth Sciences PhD, English. Université d'Orléans.

Businger, J.A., Oncley, S.P., 1990. Flux measurement with conditional sampling. J. Atmos. Oceanic Technol. 7, 349–352.

Butterbach-Bahl, K., Baggs, E.M., Dannenmann, M., Kiese, R., Zechmeister-Boltenstern, S., 2013. Nitrous oxide emissions from soils: how well do we understand the processes and their controls? Philos. Trans. R. Soc. B-Biol. Sci. 368 (1621).

Ceschia, E., et al., 2010. Management effects on net ecosystem carbon and GHG budgets at European crop sites. Agric. Ecosyst. Environ. 139 (3), 363–383.

Christiansen, J.R., Korhonen, J.F.J., Juszczak, R., Giebels, M., Pihlatie, M., 2011. Assessing the effects of chamber placement, manual sampling and headspace mixing on CH4 fluxes in a laboratory experiment. Plant Soil 343, 171–185.

Ciais, P., Sabine, C., Bala, G., Bopp, L., Brovkin, V., Canadell, J., Chhabra, A., DeFries, R., Galloway, J., Heimann, M., Jones, C., Le Quéré, C., Myneni, R.B., Piao, S., Thornton, P., 2013. Carbon and other biogeochemical cycles. In: Stocker, T.F., Qin, D., Plattner, G.-K., Tignor, M., Allen, S.K., Boschung, J., Nauels, A., Xia, Y., Bex, V., Midgley, P.M. (Eds.), Climate Change 2013: The Physical Science Basis. Contribution of Working Group I to the Fifth Assessment Report of the Intergovernmental Panel on Climate Change. Cambridge University Press, Cambridge, United Kingdom and New York, NY, USA.

Cowan, N.J., et al., 2015. Spatial variability and hotspots of soil N2O fluxes from intensively grazed grassland. Biogeosciences 12 (5), 1585–1596.

Crill, P.M., Keller, M., Weitz, A., Grauel, B., Veldkamp, E., 2000. Intensive field measurements of nitrous oxide emissions from a tropical agricultural soil. Global Biogeochem. Cycles 14 (1), 85–95.

Davidson, E.A., Savage, K., Verchot, L.V., Navarro, R., 2002. Minimizing artifacts and biases in chamber-based measurements of soil respiration. Agric. For. Meteorol. 113, 21–37.

Denmead, O., Macdonald, B., Bryant, G., Naylor, T., Wilson, S., Griffith, D., Wang, W., Salter, B., White, I., Moody, P., 2010. Emissions of methane and nitrous oxide from Australian sugarcane soils. Agric. For. Meteorol. 150, 748–756.

Deshmukh, C., Serça, D., Delon, C., Tardif, R., Demarty, M., Jarnot, C., Meyerfeld, Y., Chanudet, V., Guédant, P., Rode, W., Descloux, S., Guérin, F., 2014. Physical controls on CH_4 emissions from a newly flooded subtropical freshwater hydroelectric reservoir: nam Theun 2. Biogeosciences 11, 4251–4269.

Desjardins, R.L., et al., 2010. Multiscale estimates of N2O emissions from agricultural lands. Agric. For. Meteorol. 150 (6), 817–824.

Eugster, W., Merbold, L., 2015. Eddy covariance for quantifying trace gas fluxes from soils. Soil 1, 187–205. https://doi.org/10.5194/soil-1-187-2015.

Eugster, W., et al., 2007. Methodical study of nitrous oxide eddy covariance measurements using quantum cascade laser spectrometery over a Swiss forest. Biogeosciences 4 (5), 927–939.

Flechard, C.R., Neftel, A., Jocher, M., Ammann, C., Fuhrer, J., 2005. Bi-directional soil/atmosphere N2O exchange over two mown grassland systems with contrasting management practices. Glob. Chang. Biol. 11 (12), 2114–2127.

Foken, T., Wichura, B., 1996. Tools for quality assessment of surface-based flux measurements. Agric. For. Meteorol. 78 (1-2), 83–105.

Galle, B., Klemedtsson, L., Griffith, D.W.T., 1994. Application of a Fourier-Transform IR system for measurements of N2O fluxes using micrometeorological methods, an ultralarge chamber system, and conventional field chambers. Journal of Geophysical Research-Atmospheres 99 (D8), 16575–16583.

Hargreaves, K.J., et al., 1994. Measurement of nitrous-oxide emission from fertilized grassland using micrometeorological techniques. Journal of Geophysical Research-Atmospheres 99 (D8), 16569–16574.

Hargreaves, K.J., et al., 1996. Measurement of nitrous oxide emission from agricultural land using micrometeorological methods. Atmos. Environ. 30 (10-11), 1563–1571.

Hensen, A., Skiba, U., Famulari, D., 2013. Low cost and state of the art methods to measure nitrous oxide emissions. Environ. Res. Lett. 8 (2).

Huang, H., et al., 2014. Nitrous oxide emissions from a commercial cornfield (Zea mays) measured using the eddy covariance technique. Atmos. Chem. Phys. 14 (23), 12839–12854.

Hutchinson, G.L., Livingston, G.P., 2001. Vents and seals in non-steady-state chambers used for measuring gas exchange between soil and the atmosphere. Eur. J. Soil Sci. 52 (4), 675–682.

Hutchinson, G.L., Mosier, A.R., 1981. Improved soil cover method for field measurement of nitrous oxide fluxes. Soil Sci. Soc. Am. J. 45, 311–316.

IPCC, 2006. Emissions from livestock and manure management, in: guidelines for national greenhouse gas inventories chapter 10. Intergovernmental Panel on Climate Change. 87 pp.. http://www.ipcc-nggip.iges.or.jp/public/2006gl/pdf/4_Volume4/V4_10_Ch10_Livestock.pdf (last access: 26 February 2015).

Joly, L., et al., 2011. Development of a versatile atmospheric N2O sensor based on quantum cascade laser technology at 4.5 mu m. Appl. Phys. B-Lasers Opt. 103 (3), 717–723.

Jones, S.K., et al., 2011. Nitrous oxide emissions from managed grassland: a comparison of eddy covariance and static chamber measurements. Atmos. Meas. Tech. 4 (10), 2179–2194.

Kaimal, J.C., Finnigan, J., 1994. J.: Atmospheric Boundary Layer Flows: Their Structure and Measurement. Oxford University Press, New York, NY 289 pp.

Kormann, R., Meixner, F.X., 2001. An analytical footprint model for non-neutral stratification. Boundary. Meteorol. 99 (2), 207–224.

Kostyanovsky, K.I., Huggins, D.R., Stockle, C.O., Waldo, S., Lamb, B., 2018. Developing a flow through chamber system for automated measurements of soil N2O and CO2

emissions. Measurement 113, 172–180.
Kroon, P.S., et al., 2010. Uncertainties in eddy covariance flux measurements assessed from CH4 and N2O observations. Agric. For. Meteorol. 150 (6), 806–816.
Laville, P., Jambert, C., Cellier, P., Delmas, R., 1999. Nitrous oxide fluxes from a fertilised maize crop using micrometeorological and chamber methods. Agric. For. Meteorol. 96 (1-3), 19–38.
Lesschen, J.P., Velthof, G.L., de Vries, W., Kros, J., 2011. Differentiation of nitrous oxide emission factors for agricultural soils. Environ. Poll. 159, 3215–3222.
Liu, G., Si, B.C., 2009. Multi-layer diffusion model and error analysis applied to chamber-based gas fluxes measurements. Agric. For. Meteorol. 214, 125–132.
Mappe, I., et al., 2013. A quantum cascade laser absorption spectrometer devoted to the in situ measurement of atmospheric N2O and CH4 emission fluxes. Rev. Sci. Instrum. 84 (2).
Mappe-Fogaing, I., et al., 2012. A singular value decomposition approach for the retrieval of N2O concentrations and fluxes by quantum cascade laser absorption spectroscopy. Appl. Phys. B-Lasers Opt. 108 (4), 933–943.
Mazzetto, A.M., Barneze, A.S., Feigl, B.J., Van Groenigen, J.W., Oenema, O., Cerri, C.C., 2014. Temperature and moisture affect methane and nitrous oxide emission from bovine manure patches in tropical conditions. Soil Biol. Biochem. 76, 242–248.
Merbold, L., et al., 2014. Greenhouse gas budget (CO2, CH4 and N2O) of intensively managed grassland following restoration. Glob. Chang. Biol. 20 (6), 1913–1928.
Molodovskaya, M., Warland, J., Richards, B.K., Oberg, G., Steenhuis, T.S., 2011. Nitrous oxide from heterogeneous agricultural landscapes: source contribution analysis by Eddy Covariance and chambers. Soil Sci. Soc. Am. J. 75 (5), 1829–1838.
Moore, C.J., 1986. Frequency-response corrections for eddy-correlation systems. Boundary. Meteorol. 37 (1-2), 17–35.
Neftel, A., Flechard, C., Ammann, C., Conen, F., Emmenegger, L., Zeyer, K., 2007. Experimental assessment of N2O background fluxes in grassland systems. Tellus B 59, 470–482.
Neftel, A., et al., 2010. N2O exchange over managed grassland: application of a quantum cascade laser spectrometer for micrometeorological flux measurements. Agric. For. Meteorol. 150 (6), 775–785.
Nicolini, G., Castaldi, S., Fratini, G., Valentini, R., 2013. A literature overview of micrometeorological CH4 and N2O flux measurements in terrestrial ecosystems. Atmos. Environ. 81, 311–319.
Pattey, E., et al., 2006. Towards standards for measuring greenhouse gas fluxes from agricultural fields using instrumented towers. Can. J. Soil Sci. 86 (3), 373–400.
Pattey, E., et al., 2007. Tools for quantifying N2O emissions from agroecosystems. Agric. For. Meteorol. 142 (2-4), 103–119.
Peyrard, C., Mary, B., Perrin, P., Véricel, G., Gréhan, E., Justes, E., Léonard, J., 2016. N_2O emissions of low input cropping systems as affected by legume and cover crops use. Agric. Ecosyst. Environ. 224, 145–156.
Pihlatie, M.K., et al., 2013. Comparison of static chambers to measure CH4 emissions from soils. Agric. For. Meteorol. 171, 124–136.
Rannik, U., et al., 2015. Intercomparison of fast response commercial gas analysers for nitrous oxide flux measurements under field conditions. Biogeosciences 12 (2), 415–432.
Reinsch, T., Loges, R., Kluss, C., Taube, F., 2018. Renovation and conversion of permanent grass-clover swards to pasture or crops: effects on annual N2O emissions in the year after ploughing. Soil Tillage Res. 175, 119–129.
Rochette, P., Eriksen-Hamel, N.S., 2008. Chamber measurements of soil nitrous oxide flux: Are absolute values reliable? Soil Sci. Soc. Am. J. 72 (2), 331–342. https://doi.org/10.2136/sssaj2007.0215.
Rochette, P., Hutchinson, G.L., 2005. Measurement of soil respiration in situ: chamber techniques. In: Hatfield, J.L. (Ed.), Micrometeorology in Agricultural Systems. Agronomy Monograph. American Society of Agronomy, Madison pp. 587.
Rochette, P., McGinn, S.M., 2004. Methods for measuring soil-surface gas exchange. Soil – water – solute processes in environmental systems. Monitoring, characterization and modeling. CRC Press/Lewis Publishers Inc., Boca Raton, FL.
Shurpali, N.J., et al., 2016. Neglecting diurnal variations leads to uncertainties in terrestrial nitrous oxide emissions. Sci. Rep. 6.
Skiba, U., et al., 1996. Measurement of field scale N2O emission fluxes from a wheat crop using micrometeorological techniques. Plant Soil 181 (1), 139–144.
Smith, K.A., Dobbie, K.E., 2001. The impact of sampling frequency and sampling times on chamber-based measurements of N2O emissions from fertilized soils. Glob. Chang. Biol. 7, 933–945.
Smith, K.A., et al., 1994. Micrometeorological and chambers methods for measurement of nitrous-oxide fluxes between soils and the atmosphere - overview and conclusions. Journal of Geophysical Research-Atmospheres 99 (D8), 16541–16548.
Smith, P., Bustamante, M., Ahammad, H., Clark, H., Dong, H., Elsiddig, E.A., Haberl, H., Harper, R., House, J., Jafari, M., Masera, O., Mbow, C., Ravindranath, N.H., Rice, C.W., Robledo Abad, C., Romanovskaya, A., Sperling, F., Tubiello, F., 2014. Agriculture, forestry and other Land use (AFOLU). In: Edenhofer, O., Pichs-Madruga, R., Sokona, Y., Farahani, E., Kadner, S., Seyboth, K., Adler, A., Baum, I., Brunner, S., Eickemeier, P., Kriemann, B., Savolainen, J., Schlömer, S., von Stechow, C., Zwickel, T., Minx, J.C. (Eds.), Climate Change 2014: Mitigation of Climate Change. Contribution of Working Group III to the Fifth Assessment Report of the Intergovernmental Panel on Climate Change. Cambridge University Press, Cambridge, United Kingdom and New York, NY, USA.
Vickers, D., Mahrt, L., 1997a. Fetch limited drag coefficients. Boundary. Meteorol. 85 (1), 53–79.
Vickers, D., Mahrt, L., 1997b. Quality control and flux sampling problems for tower and aircraft data. J. Atmos. Oceanic Technol. 14 (3), 512–526.
Wang, K., et al., 2013. Comparison between static chamber and tunable diode laser-based eddy covariance techniques for measuring nitrous oxide fluxes from a cotton field. Agric. For. Meteorol. 171, 9–19.
Webb, E.K., Pearman, G.I., Leuning, R., 1980. Correction of flux measurements for density effects due to heat and water-vapor transfer. Q. J. R. Meteorol. Soc. 106 (447), 85–100.
Wichman, B.A., Hill, I.D., 1987. Building a random-number generator. BYTE 127–128.
Wienhold, F.G., Welling, M., Harris, G.W., 1995. Micrometeorological measurement and source region analysis of nitrous oxide fluxes from an agricultural soil. Atmos. Environ. 29 (17), 2219–2227.
Xu, L., Furtaw, M.D., Madsen, R.A., Garcia, R.L., Anderson, D.J., McDermitt, D.K., 2006. On maintaining pressure equilibrium between a soil CO2 flux chamber and the ambient air. J. Geophys. Res. Atmos. 111 (D8).
Zenone, T., et al., 2016. CO2 uptake is offset by CH4 and N2O emissions in a poplar short-rotation coppice. Glob. Change Biol. Bioenergy 8 (3), 524–538. https://doi.org/10.1111/gcbb.12269.
Zona, D., et al., 2013. N2O fluxes of a bio-energy poplar plantation during a two years rotation period. Glob. Change Biol. Bioenergy 5 (5), 536–547.